

On the Design of an Optimal Multi-Tone Jammer Against the Wiener Interpolation Filter

Corentin Fonteneau

Univ Rennes, INSA Rennes, IETR - UMR 6164 F-35000 Rennes, France

Abstract—In the context of civilian and military communications, anti-jamming techniques are essential to ensure information integrity in the presence of malicious interference. A conventional time-domain approach relies on computing the Wiener interpolation filter to estimate and suppress the jamming waveform from the received samples. It is widely acknowledged that this method is effective for protecting wideband systems against narrowband interference. In this work, this paradigm is questioned through the design of a K -tone jamming waveform that is intrinsically difficult to estimate assuming a L -tap Wiener interpolation filter. This design relies on an optimization procedure that maximizes the analytical Bayesian mean squared error associated with the jamming waveform estimate. Additionally, an analytical proof is provided showing that a multi-tone jamming waveform composed of $L/2 + 1$ tones is sufficient to render the Wiener-filter-based anti-jamming module completely ineffective. The analytical results are validated through Monte Carlo simulations assuming both perfect knowledge and practical estimates of the correlation functions of the received signal.

Index Terms—Narrowband interference, Multi-tone Jammer, Anti-jamming techniques, Wiener filter, Wideband system, DSSS communication.

I. INTRODUCTION

Due to the continuous and growing digitalization of human activities, information security has become a critical concern aimed at maintaining control over services and infrastructures. In this context, modern systems must guarantee both the confidentiality and the integrity of the information to be transmitted [1]–[4]. This paper focuses specifically on the latter, which characterizes the system’s ability to safeguard information from interference during transmission [2].

These interferences are commonly classified as unintentional — such as inter-carrier or co-channel interference — or intentional, when a malicious device disrupts the system [3]. This intentional disruption can take the form of a spoofing attack, in which a counterfeit signal is transmitted to mislead the receiver, or a jamming attack [4]. More specifically, the latter consists in masking the useful signal by transmitting a strong interference within the frequency band of interest. Within this framework, multiple jamming waveforms, such as pulses or chirps, have been studied in the literature with the aim of enabling the decoding of the useful information in contested environments [5]–[7].

In particular, the protection of wireless systems against narrow band interference (NBI)—often modeled as an autoregressive process of order 1 (AR(1)) or as a multi-tone

signal—has attracted significant attention over the past decades [8]–[11]. This type of interference has motivated the development of rejection techniques in the time [11], frequency [12], spatial [13], or space-time domains [14]. Regardless of the chosen domain, the underlying objective is to suppress the interference from the received signal in order to enhance the Signal-to-Interference-plus-Noise Ratio (SINR). To this end, various signal processing approaches, such as wavelet transforms [15], compressed sensing [16], Robust Principal Component Analysis (RPCA) [17], notch filtering [18] [19], and Wiener filtering [9] [20] have been investigated in different contexts.

More notably, the rejection of NBI using Wiener filtering in Direct-Sequence Spread Spectrum (DSSS) communications has been extensively discussed, as this architecture enables communication under high Jammer-to-Signal Ratio (JSR) conditions [9]–[11], [20]–[24]. In particular, the SINR is improved through both the filter gain and the inherent processing gain of the DSSS waveform. The two major advantages of the Wiener filter are, first, that it minimizes the Bayesian Mean Square Error (BMSE) of the interference estimate and, second, that it can be computed in a blind manner [11], [25]. Subsequent works on Wiener filtering introduced a multi-stage architecture, known as the Multi-Stage Wiener Filter (MSWF), which achieves the same BMSE performance at a lower computational cost through rank reduction [26]. Moreover, it requires fewer training samples to estimate the filter coefficients [27]. More recent studies have further enhanced the multi-stage framework by accelerating the convergence of the filter coefficients toward their optimal value and by improving algorithms used to select an appropriate dimension for the reduced-rank subspace [28], [29].

The combination of Wiener filtering and DSSS systems has led to extensive analytical work and numerous simulation studies on the BMSE of the interference estimate for AR(1) and multi-tone jamming waveforms [9]–[11], [20]–[24]. Specifically, closed-form expressions for the analytical BMSE have been derived for BPSK-DSSS systems subjected to a sinusoidal jammer in [21], [24] and to an AR(1) jammer in [9], [20]. Furthermore, approximations of the analytical BMSE have been provided for both BPSK-DSSS and QPSK-DSSS systems under the assumption of a sum of AR(1) jammers or a multi-tone jammer in [10]. Across these contributions, simulation results consistently indicate that substantial SINR improvements can be achieved through Wiener filtering, particularly in the presence of multi-tone jammers [11]. However,

This work has been supported in part by the project RIS3, under grant FRANCE 2030 ANR-23-CMAS-0023

these studies rely on naive multi-tone jammer models, which is a strong assumption in scenarios involving a malicious interferer. To the best of the author's knowledge, the optimization of a narrowband jamming waveform has received limited attention [23], [24]. More precisely, the authors of [23] determined the constrained-bandwidth aliased spectrum of a jammer that maximizes the BMSE, assuming an infinite-length Wiener prediction filter. Their results show that the optimal aliased spectrum depends on the aliased spectra of both the useful signal and the noise at the receiver. Finally, analytical derivations in [24] established that, for a L -tap Wiener interpolation filter and a BPSK-DSSS system, the most difficult sinusoidal jammer to estimate is obtained for the normalized angular frequency $\omega_1 = 4.493/(L + 1)$ or $\omega_1 = \pi - 4.493/(L + 1)$.

Contributions. This paper addresses the design of a multi-tone jammer that is difficult to estimate using a Wiener interpolation filter in a DSSS system. The main contributions are summarized below:

- A closed-form expression for the complex Wiener interpolation filter.
- A closed-form expression for the BMSE of the interference estimate.
- A closed-form expression for the optimal 2-tone jammer.
- A low-complexity procedure for generating the most difficult-to-estimate K -tone jammer for a L -tap filter.
- A closed-form characterization of the optimal K -tone jammer, assuming $K \geq L/2 + 1$.

Organization. The paper is organized as follows. Section II presents the system model. Section III details the analytical performance of the anti-jamming module based on the Wiener interpolation filter. Section IV discusses the design of an optimal multi-tone jamming waveform targeting this module. Section V evaluates the relevance of the proposed jamming waveforms through Monte Carlo simulations. Finally, Section VI concludes the paper.

Notations. The following notations are used in the paper : \mathbf{A} is a matrix ; \mathbf{a} is a column vector ; a is a scalar ; $[\mathbf{A}]_{ij}$ is the entry on the i th line and j th column of matrix \mathbf{A} ; \mathbf{I}_N is an $N \times N$ identity matrix ; $\mathbf{1}_N$ is a N all-ones column vector ; $\mathbf{A} = \text{diag}(a_1, \dots, a_N)$ is a $N \times N$ diagonal matrix with a_i ($1 \leq i \leq N$) elements on its diagonal diagonal matrix ; $\text{Tr}(\mathbf{A})$ is the trace of \mathbf{A} ; $(\cdot)^*$, $(\cdot)^T$, and $(\cdot)^H$ represent the conjugate, the transpose and the conjugate transpose respectively ; \mathbb{E} is the expectation symbol.

II. SYSTEM MODEL

In this section, the received signal model is detailed in II-A before the presentation of the architecture of the anti-jamming module in II-B.

A. Received signal

In this paper, a spread signal $s(t)$ is jammed by a multi-tone waveform $i(t)$ on a gaussian channel $n(t)$. The received signal $r(t)$ is sampled at chip rate under the assumption of perfect timing and frequency synchronization.

In particular, the m th interference sample i_m generated by the K -tone jammer is written,

$$i_m(\boldsymbol{\alpha}, \boldsymbol{\omega}) = \mathbf{1}_K^T \boldsymbol{\theta}_m(\boldsymbol{\alpha}, \boldsymbol{\omega}) \in \mathbb{C}, \quad (1)$$

where $\boldsymbol{\theta}_m(\boldsymbol{\alpha}, \boldsymbol{\omega}) \in \mathbb{C}^K$ is composed of the contribution of each individual tone. The contribution of the k th tone is expressed as,

$$[\boldsymbol{\theta}_m(\boldsymbol{\alpha}, \boldsymbol{\omega})]_k = \alpha_k e^{j(\omega_k m + \phi_k)} \in \mathbb{C}, \quad (2)$$

where α_k , ω_k and ϕ_k respectively represent the modulus of the complex exponential, the normalized angular frequency in $[-\pi, \pi[$ and the random initial phase that follows a uniform distribution over $[-\pi, \pi[$ for the k -th tone. Note that $\boldsymbol{\alpha} = [\alpha_1, \dots, \alpha_K]^T \in (\mathbb{R}^+)^K$ and $\boldsymbol{\omega} = [\omega_1, \dots, \omega_K]^T \in [-\pi, \pi[^K$ are the jammer parameters that will be discussed and optimized in the rest of the paper.

The m th received sample $r_m(\boldsymbol{\alpha}, \boldsymbol{\omega})$ is then written,

$$r_m(\boldsymbol{\alpha}, \boldsymbol{\omega}) = s_m + n_m + i_m(\boldsymbol{\alpha}, \boldsymbol{\omega}) \in \mathbb{C}, \quad (3)$$

where $s_m = \sqrt{S} (I_m + jQ_m) \in \mathbb{C}$ represents the m th useful sample of power S ; n_m is the m th complex additive white gaussian noise sample that follows the complex normal distribution $\mathcal{CN}(0, \sigma_n^2)$ and $i_m(\boldsymbol{\alpha}, \boldsymbol{\omega})$ is the m th jamming sample arising from the K -tone jammer of power J . It is worth noting that s_m , n_m and $i_m(\boldsymbol{\alpha}, \boldsymbol{\omega})$ are mutually uncorrelated as well as Wide Sense Stationary (WSS) processes [21].

B. General architecture of the anti-jamming module

In order to enhance the robustness of the system in contested environments, the receiver is composed of an anti-jamming module depicted in Figure 1. The estimation module produces an interference estimate $\hat{i}_m(\boldsymbol{\alpha}, \boldsymbol{\omega})$ that is expressed as,

$$\hat{i}_m(\boldsymbol{\alpha}, \boldsymbol{\omega}) = \mathbf{w}^H \mathbf{r}_m(\boldsymbol{\alpha}, \boldsymbol{\omega}) \in \mathbb{C}, \quad (4)$$

which depends on the linear interpolation filter $\mathbf{w} \in \mathbb{C}^L$ of length L and on the received samples $\mathbf{r}_m(\boldsymbol{\alpha}, \boldsymbol{\omega}) = [r_{m+L/2}, \dots, r_{m+1}, r_{m-1}, \dots, r_{m-L/2}]^T \in \mathbb{C}^L$. The estimate $\hat{i}_m(\boldsymbol{\alpha}, \boldsymbol{\omega})$ is then subtracted from $r_m(\boldsymbol{\alpha}, \boldsymbol{\omega})$ to obtain the output sample $y_m(\boldsymbol{\alpha}, \boldsymbol{\omega})$ with improved SINR, which is written,

$$y_m(\boldsymbol{\alpha}, \boldsymbol{\omega}) = r_m(\boldsymbol{\alpha}, \boldsymbol{\omega}) - \hat{i}_m(\boldsymbol{\alpha}, \boldsymbol{\omega}) \in \mathbb{C}. \quad (5)$$

At the receiver side, the main difficulty is to determine the filter \mathbf{w} that produces an accurate interference estimate. A classical solution to this problem is to find the Linear Minimum Mean Square Error (LMMSE) estimator \hat{i}^* that minimizes the power P_y of the output signal $y_m(\boldsymbol{\alpha}, \boldsymbol{\omega})$, i.e [21],

$$\mathbf{w}^* = \arg \min_{\mathbf{w}} \mathbb{E}_{s, n, \phi} [|y_m(\boldsymbol{\alpha}, \boldsymbol{\omega})|^2]. \quad (6)$$

The resolution of such a problem is equivalent to the minimization of the BMSE of the interference estimate since,

$$\begin{aligned} P_y &= \mathbb{E}_{s, n, \phi} \left[|s_m + n_m + (i_m(\boldsymbol{\alpha}, \boldsymbol{\omega}) - \hat{i}_m(\boldsymbol{\alpha}, \boldsymbol{\omega}))|^2 \right], \\ &= S + \sigma_n^2 + \text{BMSE}(\hat{i}(\boldsymbol{\alpha}, \boldsymbol{\omega})), \end{aligned} \quad (7)$$

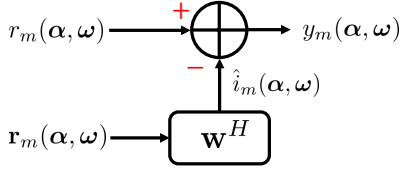


Fig. 1: Architecture of the anti-jamming module.

where,

$$\text{BMSE}(\hat{i}(\alpha, \omega)) = \mathbb{E}_{s, n, \phi} \left[|i_m(\alpha, \omega) - \hat{i}_m(\alpha, \omega)|^2 \right]. \quad (8)$$

When the processes are zero mean and WSS, as in the present case, the solution \mathbf{w}^* to this problem is commonly referred to as the Wiener filter [25]. The analytical form of \mathbf{w}^* and the BMSE of the interference estimate $\hat{i}^*(\alpha, \omega)$ are the subject of next section.

III. ANALYTICAL PERFORMANCE OF THE ANTI-JAMMING MODULE

In this section, the analytical performance of Wiener filtering in DSSS systems is studied in depth. Firstly, the complex vector form of the Wiener interpolation filter \mathbf{w}^* is analytically derived in section III-A. Then, the analytical BMSE of the interference estimate $\hat{i}^*(\alpha, \omega)$ is established in section III-B. Finally, the blind estimation of \mathbf{w}^* is discussed in section III-C.

A. Analytical solution of the Wiener interpolation filter \mathbf{w}^*

As expressed by (1), the jamming sample $i_m(\alpha, \omega)$ is a sum of K unknown jamming samples $[\theta_m(\alpha, \omega)]_k$ given by (2). Reminding that the LMMSE estimator of a sum of unknown parameters is the sum of the individual estimators, the interference estimate $\hat{i}_m^*(\alpha, \omega)$ is written [25, P390],

$$\hat{i}_m^*(\alpha, \omega) = \mathbf{1}_K^T \hat{\theta}_m^*(\alpha, \omega), \quad (9)$$

where $\hat{\theta}_m^*(\alpha, \omega) = [\hat{\theta}_m^*(\alpha_1, \omega_1), \dots, \hat{\theta}_m^*(\alpha_K, \omega_K)]^T \in \mathbb{C}^K$ consists of one estimate per tone. As samples are zero mean and WSS, $\hat{\theta}_m^*(\alpha, \omega)$ is written [25, eq.(12.20)],

$$\hat{\theta}_m^*(\alpha, \omega) = \mathbf{C}_{r\theta}^H(\alpha, \omega) \mathbf{C}_{rr}^{-1}(\alpha, \omega) \mathbf{r}_m(\alpha, \omega), \quad (10)$$

where $\mathbf{C}_{rr}(\alpha, \omega) \in \mathbb{C}^{L \times L}$ and $\mathbf{C}_{r\theta}(\alpha, \omega) \in \mathbb{C}^{L \times K}$ respectively denote the covariance matrix and the cross-covariance matrix for L observations and K unknown parameters. From (4), (9) and (10), the analytical expression of the complex Wiener interpolation filter \mathbf{w}^* can be determined in the special case of a multi-tone jammer in DSSS systems. This is the subject of Theorem 1:

Theorem 1. *The Wiener interpolation filter \mathbf{w}^* for a multi-tone jammer in DSSS systems is expressed as,*

$$\mathbf{w}^* = \mathbf{C}_{rr}^{-1}(\alpha, \omega) \mathbf{C}_{r\theta}(\alpha, \omega) \mathbf{1}_K \in \mathbb{C}^K, \quad (11)$$

where,

$$\mathbf{C}_{rr}(\alpha, \omega) = (S + \sigma_n^2) \mathbf{I}_L + \Psi(\omega) \mathbf{J}(\alpha) \Psi^H(\omega) \in \mathbb{C}^{L \times L}, \quad (12)$$

$$\mathbf{C}_{r\theta}(\alpha, \omega) = \Psi(\omega) \mathbf{J}(\alpha) \in \mathbb{C}^{L \times K}, \quad (13)$$

$$\mathbf{J}(\alpha) = \text{diag}(\alpha_1^2, \alpha_2^2, \dots, \alpha_K^2) \in (\mathbb{R}^+)^{K \times K}, \quad (14)$$

$$\Psi(\omega) = [\psi(\omega_1), \psi(\omega_2), \dots, \psi(\omega_K)] \in \mathbb{C}^{L \times K}, \quad (15)$$

$$\psi(\omega_k) = \left[e^{j\frac{L}{2}\omega_k}, \dots, e^{j\omega_k}, e^{-j\omega_k}, \dots, e^{-j\frac{L}{2}\omega_k} \right]^T \in \mathbb{C}^L. \quad (16)$$

Proof. Appendix A □

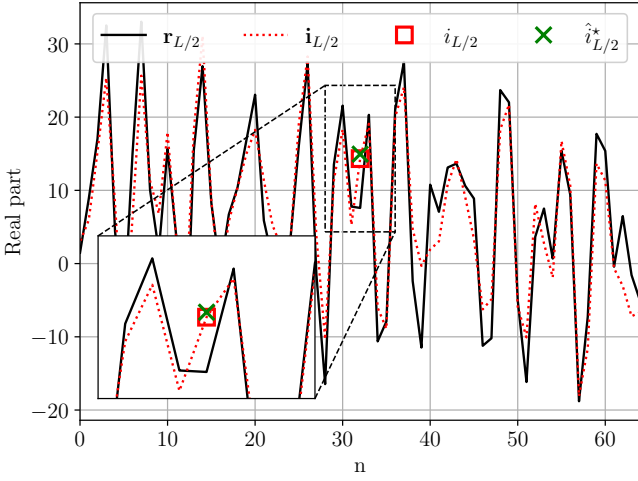
As an example, the estimation of a 4-tone jammer is qualitatively studied, assuming perfect knowledge of the matrices $\mathbf{C}_{rr}(\alpha, \omega)$ and $\mathbf{C}_{r\theta}(\alpha, \omega)$ in a QPSK-DSSS system characterized by a Signal-to-Noise Ratio (SNR) of -15 dB and a JSR of 25 dB.

Specifically, Figures 2a and 2b show that the interference estimate $\hat{i}_{L/2}^*(\alpha, \omega)$, obtained by applying (4) and (11), closely matches both the real part and imaginary parts of the complex jamming sample $i_{L/2}(\alpha, \omega)$ for a filter length $L = 64$. Additionally, Figure 2c depicts the interference estimate $[\hat{\theta}_{L/2}^*(\alpha, \omega)]_k$ for each tone, as well as the resulting multi-tone estimate $\hat{i}_{L/2}^*(\alpha, \omega)$, assuming a fixed scenario $\{\alpha, \omega, \phi\}$ over multiple random realizations of the useful signal $\mathbf{s}_{L/2}$ and the additive white gaussian noise $\mathbf{n}_{L/2}$. This illustration highlights that, even with perfect knowledge of the matrices $\mathbf{C}_{rr}(\alpha, \omega)$ and $\mathbf{C}_{r\theta}(\alpha, \omega)$, the error in the interference estimate $\hat{i}_{L/2}^*(\alpha, \omega)$ depends on the specific realizations of $\mathbf{s}_{L/2}$ and $\mathbf{n}_{L/2}$. Finally, the Figure 2d depicts that the Probability Density Function (PDF) of the interference estimate is sensitive to the length L of the Wiener interpolation filter, i.e, to the number of samples that are available for interference estimation. As shown in the figure, the higher the value of L , the lower the dispersion and the better the quality of the estimate $\hat{i}_{L/2}^*(\alpha, \omega)$.

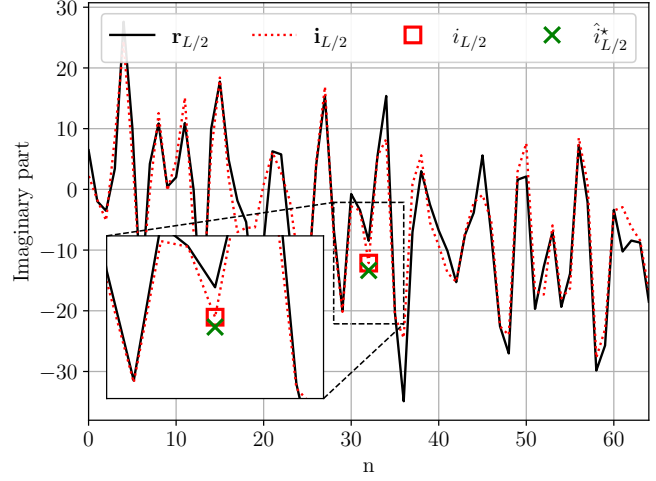
This preliminary qualitative analysis on the estimation error is complemented in section III-B by the analytical derivation of the BMSE of the interference estimate $\hat{i}^*(\alpha, \omega)$, obtained for a fixed jamming scenario $\{\alpha, \omega\}$ under random realizations $\{\phi, \mathbf{s}, \mathbf{n}\}$.

B. Analytical BMSE of the interference estimate $\hat{i}^*(\alpha, \omega)$

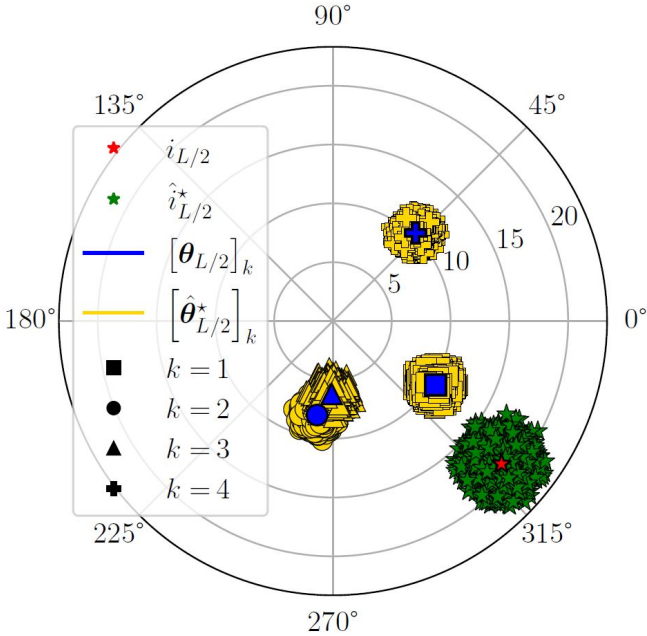
The BMSE of the interference estimate $\hat{i}^*(\alpha, \omega)$ is a key metric for the interference suppression problem, as it quantifies the quality of the interference estimation and, consequently, the suppression capability of the anti-jamming module. This is the subject of Theorem 2:



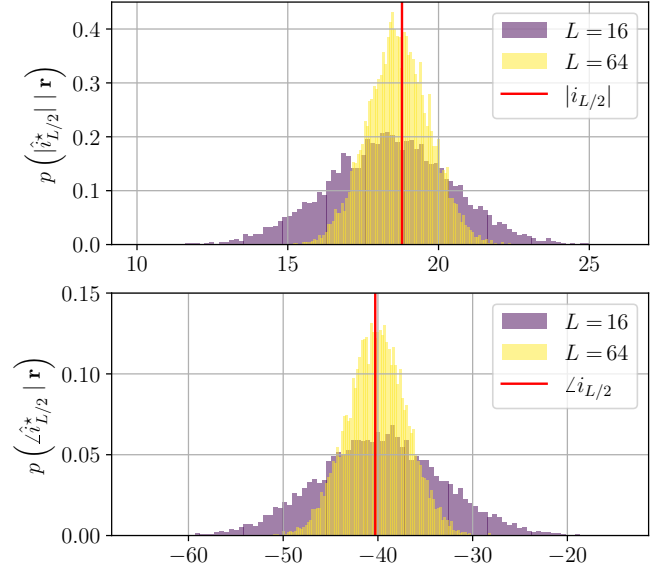
(a) Estimation of the real part of the interference for $L = 64$.



(b) Estimation of the imaginary part of the interference for $L = 64$.



(c) Estimation of the individual interfering tones $\theta_{L/2}$ and of the resulting jamming sample $i_{L/2}$, assuming various random draws of $s_{L/2}$ and $n_{L/2}$ for a fixed scenario $\{\alpha, \omega, \phi\}$.



(d) PDF of the module and phase of the estimated interference $\hat{i}_{L/2}^*$ with respect to the filter length L of the Wiener interpolation, assuming various random draws of $s_{L/2}$ and $n_{L/2}$ for a fixed scenario $\{\alpha, \omega, \phi\}$.

Fig. 2: Estimation of a 4-tone jammer in a QPSK-DSSS system by Wiener filtering ($SNR = -15$ dB, $JSR = 25$ dB).

Theorem 2. The BMSE of the interference estimate $\hat{i}^*(\alpha, \omega)$ for a multi-tone jammer in DSSS systems is expressed as,

$$\text{BMSE}(\hat{i}^*(\alpha, \omega)) = \mathbf{1}_K^T \mathbf{C}_\epsilon^*(\alpha, \omega) \mathbf{1}_K, \quad (17)$$

with,

$$\mathbf{C}_\epsilon^*(\alpha, \omega) = \mathbf{A}^{-1}(\alpha, \omega) \mathbf{J}(\alpha) \in \mathbb{R}^{K \times K}, \quad (18)$$

$$\mathbf{A}(\alpha, \omega) = \mathbf{I}_K + (S + \sigma_n^2)^{-1} \mathbf{J}(\alpha) \mathbf{\Gamma}(\omega) \in \mathbb{R}^{K \times K}, \quad (19)$$

$$\mathbf{\Gamma}(\omega) = \mathbf{\Psi}^H(\omega) \mathbf{\Psi}(\omega) \in \mathbb{R}^{K \times K} \quad (20)$$

$$[\mathbf{\Gamma}(\omega)]_{kk'} = D_{L/2}(\Delta_{k'k}) - 1 \in \mathbb{R}, \quad (21)$$

where $\mathbf{C}_\epsilon^*(\alpha, \omega)$ is the minimum error covariance matrix, $\Delta_{k'k} = w_{k'} - w_k$ is the normalized angular frequency difference between the k' th tone and the k th one, and

$D_n(x) = \sin((n+1/2)x)/\sin(x/2)$ denotes the n th Dirichlet kernel.

Proof. Appendix B \square

This theorem highlights that the BMSE of the interference estimate $\hat{i}^*(\alpha, \omega)$ depends not only on the BMSEs of individual tone estimates, i.e. $[\mathbf{C}_\epsilon^*(\alpha, \omega)]_{kk} = \text{BMSE}(\hat{\theta}^*(\alpha_k, \omega_k))$, but also on the correlation of the estimation errors, i.e. $[\mathbf{C}_\epsilon^*(\alpha, \omega)]_{kk'}, k \neq k'$. The design method introduced in Section IV exploits this property to generate a multi-tone jamming waveform that is difficult to estimate.

C. Blind estimation of the Wiener interpolation filter \mathbf{w}^*

Before discussing the design of the multi-tone jammer in the next section, the blind estimation of the Wiener interpolation filter \mathbf{w}^* is addressed as this approach is exploited in Section V to obtain the numerical results.

First, it's worth noting that the term $\mathbf{C}_{r\theta}(\alpha, \omega)\mathbf{1}_K$ (11) can be rewritten solely in terms of the received signal. Indeed,

$$\begin{aligned} \mathbf{C}_{r\theta}(\alpha, \omega)\mathbf{1}_K &= \mathbb{E}_{s, n, \phi} [\mathbf{r}_m(\alpha, \omega)\theta_m^H(\alpha, \omega)] \mathbf{1}_K, \\ &= \mathbb{E}_{s, n, \phi} [\mathbf{r}_m(\alpha, \omega)i_m^*(\alpha, \omega)], \\ &= \mathbf{c}_{ri}(\alpha, \omega), \\ &= \mathbb{E}_{s, n, \phi} [\mathbf{r}_m(\alpha, \omega, \phi)r_m^*(\alpha, \omega)]. \end{aligned} \quad (22)$$

Consequently, the matrix $\mathbf{C}_{rr}(\alpha, \omega)$ and the vector $\mathbf{c}_{ri}(\alpha, \omega)$ can be directly estimated from the received signal [11], [29],

$$\hat{\mathbf{C}}_{rr}(\alpha, \omega) = \frac{1}{M} \sum_{m=L/2}^{L/2+M-1} \mathbf{r}_m(\alpha, \omega)\mathbf{r}_m^H(\alpha, \omega), \quad (23)$$

$$\hat{\mathbf{c}}_{ri}(\alpha, \omega) = \frac{1}{M} \sum_{m=L/2}^{L/2+M-1} \mathbf{r}_m(\alpha, \omega)r_m^*(\alpha, \omega), \quad (24)$$

where $\hat{\mathbf{C}}_{rr}(\alpha, \omega)$, $\hat{\mathbf{c}}_{ri}(\alpha, \omega)$ and M respectively denote the estimate of the covariance matrix of the received samples, the estimate of the cross-covariance vector between the received samples and the interference, and the number of L -size vector used for the computation. Once (23) and (24) are computed, \mathbf{w}^* is obtained by multiplying the inverse of $\hat{\mathbf{C}}_{rr}(\alpha, \omega)$ to $\hat{\mathbf{c}}_{ri}(\alpha, \omega)$.

IV. DESIGN OF AN OPTIMAL MULTI-TONE JAMMER

In this section, the design of an optimal multi-tone jammer against the Wiener interpolation filter is investigated. First, the optimization problem is formulated in section IV-A. The problem is then analyzed and solved for $K = 1$ tone in section IV-B, for $K = 2$ tones in section IV-C, for $3 \leq K < \frac{L}{2} + 1$ tones in section IV-D, and for $K \geq \frac{L}{2} + 1$ in section IV-E.

A. Optimization problem

Assuming that the receiver embeds an anti-jamming module based on the Wiener interpolation filter \mathbf{w}^* , the jammer's goal is to maximize the BMSE of the interference estimate $\hat{i}^*(\alpha, \omega)$

(17). Recalling that the jammer power at the receiver is J , the optimization problem can be formulated as,

$$\begin{aligned} &\underset{\alpha, \omega}{\text{minimize}} \quad f(\alpha, \omega) = -\text{BMSE}(\hat{i}^*(\alpha, \omega)), \\ &\text{subject to } \|\alpha\|_2^2 = J \end{aligned} \quad (25)$$

where $f(\alpha, \omega)$ denotes the loss function. The following subsections discuss the minimization of this function with respect to the number of jamming tones K .

B. Optimization for $K = 1$ tone

For a jamming waveform composed of $K = 1$ tone, the modulus α_1 equals \sqrt{J} to satisfy the power constraint. The BMSE of the interference estimate $\hat{i}^*(\sqrt{J}, \omega_1)$ is the subject of Corollary 2.1:

Corollary 2.1. *The BMSE of the interference estimate $\hat{i}^*(\sqrt{J}, \omega_1)$ for a 1-tone jamming waveform is expressed as,*

$$\text{BMSE}(\hat{i}^*(\sqrt{J}, \omega_1)) = \frac{S + \sigma_n^2}{\frac{S + \sigma_n^2}{J} + L}. \quad (26)$$

Proof. Noticing that $\Gamma(\omega_1) = L$ and $\mathbf{J}(\sqrt{J}) = J$, (26) is directly obtained from (17) to (19). \square

From Corollary 2.1, it is figured out that the BMSE of the interference estimate $\hat{i}^*(\sqrt{J}, \omega_1)$ does not depend on the optimization variable ω_1 . Consequently, the interference estimate can only be degraded by increasing the jammer power J .

C. Optimization for $K = 2$ tones

In order to determine the optimal 2-tone jammer, the original problem (25) is reformulated as follows,

$$\underset{\alpha, \omega, \lambda}{\text{minimize}} \quad \mathcal{L}(\alpha, \omega, \lambda) = f(\alpha, \omega) + \lambda \left(-J + \sum_{k=1}^K \alpha_k^2 \right), \quad (27)$$

where $\mathcal{L}(\alpha, \omega, \lambda)$ and λ respectively denote the Lagrangian function and the Lagrange multiplier. To solve (27), the partial derivatives of $\mathcal{L}(\alpha, \omega, \lambda)$ with respect to ω_k and α_k^2 are first calculated regardless the value of K . This is the subject of Theorem 3:

Theorem 3. *The partial derivative of the Lagrangian function $\mathcal{L}(\alpha, \omega, \lambda)$ with respect to α_k^2 is,*

$$\frac{\partial \mathcal{L}(\alpha, \omega, \lambda)}{\partial \alpha_k^2} = -(\mathbf{1}_K^T \mathbf{e}_k)^2 + \lambda, \quad (28)$$

$$\mathbf{E}(\alpha, \omega) = [\mathbf{e}_1, \dots, \mathbf{e}_k, \dots, \mathbf{e}_K] = \mathbf{A}^{-1}(\alpha, \omega), \quad (29)$$

and the partial derivative of the Lagrangian function $\mathcal{L}(\alpha, \omega, \lambda)$ with respect to ω_k is,

$$\frac{\partial \mathcal{L}(\alpha, \omega, \lambda)}{\partial \omega_k} = \frac{\mathbf{1}_K^T}{S + \sigma_n^2} \mathbf{C}_\epsilon(\alpha, \omega) \frac{\partial \Gamma(\omega)}{\partial \omega_k} \mathbf{C}_\epsilon(\alpha, \omega) \mathbf{1}_K, \quad (30)$$

$$\left[\frac{\partial \Gamma(\omega)}{\partial \omega_k} \right]_{kk'} = \left[\frac{\partial \Gamma(\omega)}{\partial \omega_k} \right]_{k'k} = \begin{cases} \frac{\partial D_{L/2}(\Delta_{k'k})}{\partial \omega_k}, k \neq k' \\ 0 \text{ elsewhere} \end{cases}, \quad (31)$$

$$\frac{\partial D_{L/2}(\Delta_{k'k})}{\partial \omega_k} = \left[\frac{1}{2} \sin \left((L+1) \frac{\Delta_{k'k}}{2} \right) \cos \left(\frac{\Delta_{k'k}}{2} \right) - \frac{L+1}{2} \cos \left((L+1) \frac{\Delta_{k'k}}{2} \right) \sin \left(\frac{\Delta_{k'k}}{2} \right) \right] / \sin^2 \left(\frac{\Delta_{k'k}}{2} \right). \quad (32)$$

Proof. Appendix C \square

From partial derivatives $\partial \mathcal{L}(\alpha, \omega, \lambda) / \partial \alpha_k^2$ and $\partial \mathcal{L}(\alpha, \omega, \lambda) / \partial \omega_k$, the convexity of the Lagrangian function $\mathcal{L}(\alpha, \omega, \lambda)$ is studied for $K = 2$ and the optimal solution with regard to L is determined. This is the subject of Proposition 1:

Proposition 1. *The 2-tone jammer that maximizes the BMSE of the interference estimate is parameterized as follows,*

$$\alpha^\dagger = \left[\sqrt{J/2}, \sqrt{J/2} \right]^T, \quad (33)$$

$$\omega^\dagger = \left[\omega_1, \omega_1 + \Delta_{21}^\dagger \right]^T, \quad (34)$$

$$\Delta_{21}^\dagger = \begin{cases} 9/(L+1) \\ 2\pi - 9/(L+1) \end{cases}. \quad (35)$$

The BMSE obtained for this jamming waveform is expressed as,

$$\text{BMSE} \left(\hat{i}^*(\alpha^\dagger, \omega^\dagger) \right) = \frac{S + \sigma_n^2}{\frac{S + \sigma_n^2}{J} + \frac{L-1}{2} + \frac{D_{L/2}(\Delta_{21}^\dagger)}{2}}. \quad (36)$$

Proof. Appendix D \square

First, it is pointed out from (33) to (35) that there is an infinite number of optimal 2-tone jammers rather than a single one. These jammers share the common characteristics of being composed of two equal-power tones, whose normalized angular frequency difference equals Δ_{21}^\dagger . Consequently, in accordance with (36), the absolute frequency positions of these tones have no impact on the BMSE of the interference estimate $\hat{i}^*(\alpha^\dagger, \omega^\dagger)$. Finally, it is worth noting from (26) and (36) that, regardless of Δ_{21} , a jammer composed of two equal-power tones is intrinsically harder to estimate than its 1-tone counterpart as $D_{L/2}(\Delta_{21}) \leq L+1$.

D. Optimization for $3 \leq K < \frac{L}{2} + 1$ tones

The resolution of problem (25) requires the inversion of matrix $\mathbf{A}(\alpha, \omega) \in \mathbb{R}^{K \times K}$, thereby complicating the analytical derivation of the optimal jammer for $3 \leq K < \frac{L}{2} + 1$. Therefore, a gradient-based optimization algorithm is employed to iteratively compute α and ω . The general update rule at the i th iteration is given by,

$$\begin{cases} \alpha_{(i)} = \mathcal{P}_{\mathcal{S}}(\alpha_{(i-1)} - \mu_\alpha \nabla_\alpha f(\alpha_{(i-1)}, \omega_{(i-1)})) \\ \omega_{(i)} = \omega_{(i-1)} - \mu_\omega \nabla_\omega f(\alpha_{(i-1)}, \omega_{(i-1)}) \end{cases}, \quad (37)$$

where the projection operator $\mathcal{P}_{\mathcal{S}}(\alpha) = \sqrt{J} \times \alpha / \|\alpha\|_2$ ensures that the power constraint is satisfied after each iteration, and μ_α (resp. μ_ω) denotes the step size associated with α (resp. ω). In practice, the optimization process is initialized using multiple pairs of random initial vectors $\{\alpha_{(0)}^r, \omega_{(0)}^r\}$ and the resulting solution $\{\alpha_{\text{opt}}^r, \omega_{\text{opt}}^r\}$ that minimizes $f(\alpha, \omega)$ at convergence is selected to generate the jamming waveform. Nevertheless, this method can be computationally relaxed by properly selecting the initial pair $\{\alpha_{(0)}, \omega_{(0)}\}$.

To this end, it is first noted that the proposition 1 gives the optimal difference Δ_{21}^\dagger that jointly maximizes the BMSE of individual tone estimates, i.e. $[\mathbf{C}_\epsilon^*(\alpha^\dagger, \omega^\dagger)]_{11} = \text{BMSE}(\hat{\theta}^*(\alpha_1^\dagger, \omega_1^\dagger))$ and $[\mathbf{C}_\epsilon^*(\alpha^\dagger, \omega^\dagger)]_{22} = \text{BMSE}(\hat{\theta}^*(\alpha_2^\dagger, \omega_2^\dagger))$, as well as the correlation of the estimation errors, i.e. $[\mathbf{C}_\epsilon^*(\alpha^\dagger, \omega^\dagger)]_{12}$ and $[\mathbf{C}_\epsilon^*(\alpha^\dagger, \omega^\dagger)]_{21}$. Following the same waveform design philosophy, $\alpha_{(0)}$ and $\omega_{(0)}$ are chosen such that the jamming tones are equally powered and spaced by Δ_{21}^\dagger to penalize both the BMSE of individual tone estimates $[\mathbf{C}_\epsilon^*(\alpha^\dagger, \omega^\dagger)]_{kk}$ and the correlation of estimation errors linked to adjacent tones, i.e. $[\mathbf{C}_\epsilon^*(\alpha^\dagger, \omega^\dagger)]_{kk-1}$ and $[\mathbf{C}_\epsilon^*(\alpha^\dagger, \omega^\dagger)]_{kk+1}$. This leads to the following parameterization,

$$\alpha_{(0)}^\dagger = \sqrt{J/K} \times \mathbf{1}_K^T, \quad (38)$$

$$[\omega_{(0)}^\dagger]_k = \omega_1 + (k-1) \times \Delta_{21}^\dagger, \quad (39)$$

with $\Delta_{21}^\dagger = 9/(L+1)$, where the initial pair $\{\alpha_{(0)}^\dagger, \omega_{(0)}^\dagger\}$ is expected to be in the vicinity of the global minimum of the function $f(\alpha, \omega)$. However, this solution ignores the fact that a correlation exists between estimation errors linked to non-adjacent tones. To address this issue, it is proposed to refine the jamming waveform by solely updating the vector $\omega_{(i)}^\dagger$ with a per-tone correction term Δ_k^{opt} , which is obtained via gradient-based optimization. This leads to the solution,

$$[\omega_{\text{opt}}^\dagger]_k = [\omega_{(0)}^\dagger]_k + \Delta_k^{\text{opt}}, \quad (40)$$

where Δ_k^{opt} denotes the correction term associated with the k th tone. In the rest of the paper, the Adam optimizer is used to obtain $\{\alpha_{\text{opt}}^r, \omega_{\text{opt}}^r\}$ and $\omega_{\text{opt}}^\dagger$ [30]. The initial learning rates μ_α and μ_ω are set to 5×10^{-2} and 10^{-2} respectively, and the maximum number of iterations is parameterized to 10^3 .

Firstly, the hypothesis that the correction term Δ_k^{opt} mainly increases the correlation of estimation errors linked to non-adjacent tones is assessed in Figure 3 for jamming waveforms composed of $K = 3$ to $K = 8$ tones, assuming a 16-tap filter. The following metrics are introduced for this evaluation,

$$R = \frac{N}{D} = \frac{\text{BMSE}(\hat{i}^*(\alpha_{(0)}^\dagger, \omega_{\text{opt}}^\dagger))}{\text{BMSE}(\hat{i}^*(\alpha_{(0)}^\dagger, \omega_{(0)}^\dagger))}, \quad (41)$$

$$R_0 = \frac{N_0}{D_0} = \frac{\text{Tr}(\mathbf{C}_\epsilon^*(\alpha_{(0)}^\dagger, \omega_{\text{opt}}^\dagger))}{\text{Tr}(\mathbf{C}_\epsilon^*(\alpha_{(0)}^\dagger, \omega_{(0)}^\dagger))}, \quad (42)$$

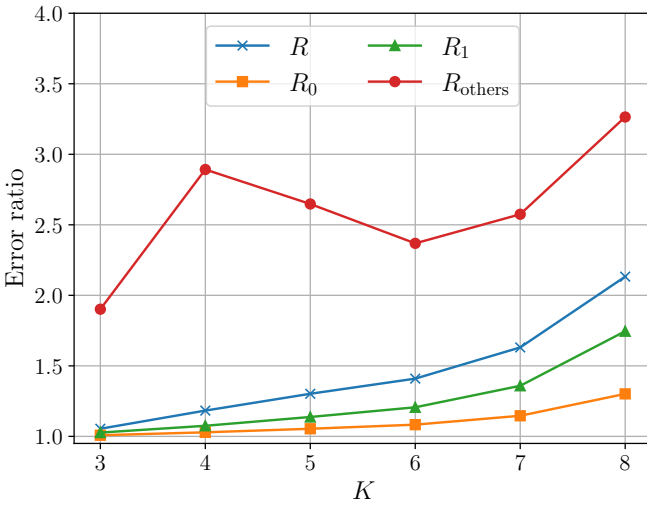


Fig. 3: Increase in error ratio obtained with the help of the optimizer.

$$R_1 = \frac{N_1}{D_1} = \frac{\sum_{k=1}^{K-1} \left[\mathbf{C}_\epsilon^*(\alpha_{(0)}^\dagger, \omega_{(0)}^\dagger) \right]_{k(k+1)}}{\sum_{k=1}^{K-1} \left[\mathbf{C}_\epsilon^*(\alpha_{(0)}^\dagger, \omega_{(0)}^\dagger) \right]_{k(k+1)}}, \quad (43)$$

$$R_{\text{others}} = \frac{N - N_0 - 2N_1}{D - D_0 - 2D_1}, \quad (44)$$

where R , R_0 , R_1 and R_{others} respectively denote the increase in error ratio obtained with the help of the optimizer for the BMSE of the interference estimate \hat{i}^* (41), for the BMSE of individual tone estimates $\hat{\theta}_k^*$ (42), for the correlation of estimation errors related to adjacent tones (43) and for the correlation of estimation errors related to non-adjacent tones (44). As observed in Figure 3, the error ratio R_{others} is greatly improved by the optimization process, which confirms the relevance of the additional term Δ_k^{opt} to increase the correlation of estimation errors related to non-adjacent tones. More moderate gains are obtained for R_0 and R_1 , which attests that the initial point $\{\alpha_{(0)}^\dagger, \omega_{(0)}^\dagger\}$ is an efficient way of penalizing both the BMSE of individual tone estimates $\hat{\theta}_k^*$ and the correlation of estimation errors linked to adjacent tones.

Finally, the optimization process of solutions $\{\alpha_{\text{opt}}^r, \omega_{\text{opt}}^r\}$ and $\{\alpha_{(0)}^\dagger, \omega_{\text{opt}}^\dagger\}$ is depicted in Figure 4, in which the normalized objective function $f(\alpha, \omega)$ is represented with respect to the number of iterations of the optimizer. Initial vectors $\{\alpha_{(0)}^r, \omega_{(0)}^r\}$ are randomly drawn from uniform distributions. As observed in this figure, the optimization process associated to $\{\alpha_{(0)}^\dagger, \omega_{\text{opt}}^\dagger\}$ has the advantage of converging faster to the global minima and makes optimization of multiple initial points useless, which is desirable from a complexity point of view.

E. Optimization for $K \geq \frac{L}{2} + 1$ tones

No more optimization process is needed for $K \geq \frac{L}{2} + 1$ tones. This is the subject of Proposition 2:

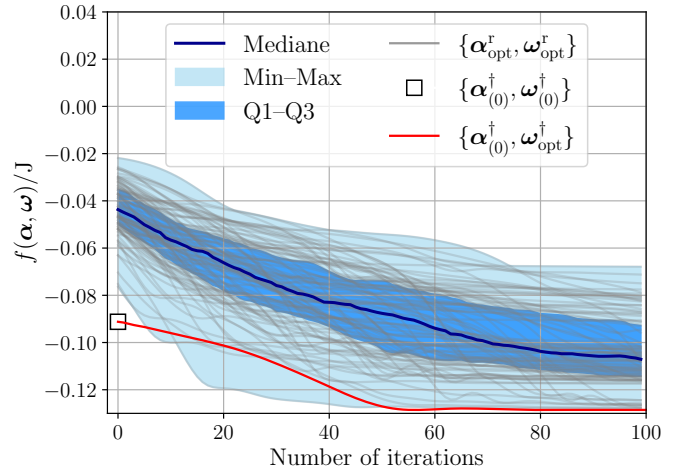


Fig. 4: Jamming waveform optimisation for $K = 6$ tones and $L = 16$.

Proposition 2. A K -tone jammer which is parameterized as follows,

$$\alpha^\ddagger = \sqrt{J/K} \times \mathbf{1}_K^T, \quad (45)$$

$$[\omega^\ddagger]_k = \omega_1 + (k-1) \times \frac{2\pi}{K}, \quad (46)$$

leads to the following BMSE for the interference estimate $\hat{i}^*(\alpha^\ddagger, \omega^\ddagger)$,

$$\text{BMSE} \left(\hat{i}^*(\alpha^\ddagger, \omega^\ddagger) \right) = \left[J^{-1} + \frac{2}{S + \sigma_n^2} \left\lfloor \frac{L}{2K} \right\rfloor \right]^{-1}. \quad (47)$$

This parameterization becomes optimal for $K \geq \frac{L}{2} + 1$ tones as $\text{BMSE} \left(\hat{i}^*(\alpha^\ddagger, \omega^\ddagger) \right) = J$.

Proof. Appendix E □

First, it is pointed out from (47) that increasing the number of tones does not always mean improving the jammer performance. Indeed, two K -tone jammers with equal ratio $\lfloor \frac{L}{2K} \rfloor$ will perform the same. Additionally, in contested environments for which $J \gg (S + \sigma_n^2)$ holds, it becomes almost ineffective to further increase the jammer power J in order to enlarge the BMSE when $K < L/2 + 1$. This behavior is explained by the fact that the BMSE in (47) is dominated by the leading term $\frac{2}{(S + \sigma_n^2)} \lfloor \frac{L}{2K} \rfloor$ in the denominator, making the jamming waveform poorly effective. On the contrary, the jamming waveform becomes highly effective when $K \geq \frac{L}{2} + 1$ tones. In this case, the BMSE equals J , indicating that this jamming waveform constitutes an optimal solution to (25) as the anti-jamming module no longer provides any suppression capability. Last but not least, this result highlights that a jammer can choose K in order to make all the anti-jamming modules based on a Wiener interpolation filter of length $L \leq 2(K-1)$ completely ineffective.

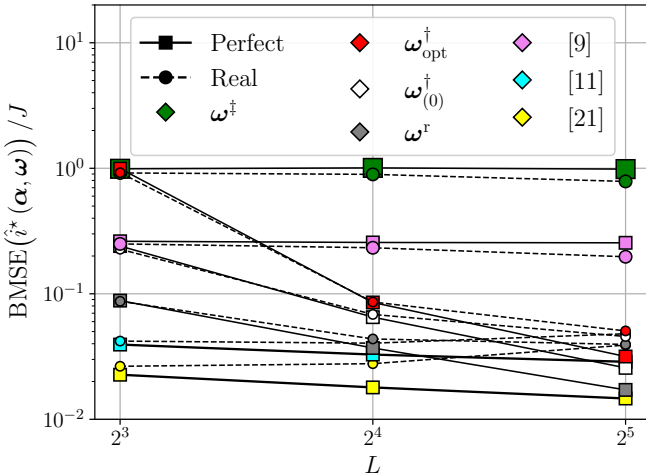


Fig. 5: Empirical BMSE of the interference estimate ($SNR = -15$ dB, $JSR = 25$ dB).

V. SIMULATION RESULTS

In this section, the efficiency of the suggested jamming waveform design is assessed by performing a Monte-Carlo simulation for a receiver embedding a Wiener interpolation filter \mathbf{w}^* of length $L \in \{8, 16, 32\}$ in a QPSK-DSSS scenario. The normalized BMSE of the interference estimate $\hat{i}^*(\alpha, \omega)$ is depicted in Figure 5 for various jamming waveforms, which are detailed in the next paragraph. Whatever the jamming waveform, the filter \mathbf{w}^* is computed assuming either a perfect knowledge of $\mathbf{C}_{rr}(\alpha, \omega)$ (12) and $\mathbf{C}_{r\theta}(\alpha, \omega)$ (13) or the real estimates $\hat{\mathbf{C}}_{rr}(\alpha, \omega)$ (23) and $\hat{\mathbf{c}}_{ri}(\alpha, \omega)$ (24). In the latter case, these estimates are computed in a limited time window of $N = 128$ samples, with $M = N - L$. This choice has been made as it is important to restrict the value N in practice to ensure that the anti-jamming module can adapt to possible changes of the jamming waveform [11].

Six equal-power tones jamming waveforms are compared. Three of them come from the jamming waveform design suggested in section IV: a 5-tone jammer parameterized by $\omega_{(0)}^\dagger$ (39), a 5-tone jammer parameterized by $\omega_{\text{opt}}^\dagger$ (40) and a $(L/2 + 1)$ -tone jammer parameterized by ω^\dagger (46). The three others directly come from the literature: an equally spaced 100-tone jammer spanning 20% of the bandwidth [11], an equally spaced 10-tone jammer with an interval of 3.6 degrees between adjacent tones [21] and a 5-tone jammer ω^r for which the angular frequencies are randomly drawn from an uniform distribution between $-\pi$ and π . Note that the latter approach aims to represent articles for which the chosen angular frequencies are given without being discussed [19]. Additionally, a seventh jamming waveform, based on an AR(1) process, is considered as this approach has been shown to be more effective than multiband jamming [9], [20]. The covariance sequence of this jamming waveform is given by $\rho_k = J \times \alpha^{|k|}$ and $\alpha = 0.8$ has been chosen to be in line with [9].

First, the performance of jammers is analyzed assuming perfect knowledge of correlation functions. It is observed that the jamming approaches considered in [11] and [21] are poorly effective as less than 4% of the jammer power remains after the anti-jamming module. The random jammer ω^r composed of 5 tones is slightly more effective than the latter approaches for $L = 8$ but becomes less and less effective as L increases. This result indicates that, when L is high compared to K , it is more effective to jam a portion of the bandwidth with a sufficient density of tones, as suggested by [11] and [21], rather than random frequency components. As expected, the AR(1) jammer is much more effective with a residual power that equals 30% of the jammer power after the anti-jamming module. Interestingly, this last approach is matched by the 5-tone jammer with the analytical parameterization $\omega_{(0)}^\dagger$ and surpassed by the parameterization $\omega_{\text{opt}}^\dagger$ obtained after optimization for $L = 8$. Note that the residual power obtained with the latter reaches 100% of the jammer power, indicating that the anti-jamming module becomes completely ineffective. However, the jammer efficiency of such approaches decreases significantly as L increases since the number of tones K is insufficient. This analysis is confirmed by the performance of the jammer parameterized by ω^\dagger which ensures the ineffectiveness of the anti-jamming-module regardless of L by being defined over a sufficiently large number of tones, namely $K = L/2+1$.

Second, the performance of jammers is studied assuming real estimates of correlation functions. With the exception of ω^\dagger , it is observed that the BMSE is slightly higher than the one obtained with the perfect knowledge counterpart whatever the jamming parameterization. This result indicates that the quality of the interference estimation is degraded by the partial knowledge of the correlation functions, which in turn reduces the performance of the anti-jamming module. Conversely, partial knowledge of these functions can be beneficial from the receiver's perspective when the jammer is parameterized by ω^\dagger , since this jamming approach is optimal under perfect knowledge of the correlation functions.

These results highlight that the jamming waveform design detailed in section IV provides an efficient solution against the Wiener interpolation filter, under perfect knowledge or real estimates of the correlation functions. Last but not least, these results illustrate how the filter length L is a sensitive information for the receiver security since the number of tones K can be adapted to make the anti-jamming module completely ineffective.

VI. CONCLUSION

In this paper, a method for generating the most difficult-to-estimate K -tone jammer for a L -tap Wiener interpolation filter is proposed. The core principle of this method is to maximize the BMSE of the jamming waveform estimate produced by the Wiener interpolation filter. To this end, closed-form expressions of both the Wiener interpolation filter and the BMSE of the multi-tone estimate are derived analytically. Based on these expressions, the optimal two-tone jammer is obtained in closed

form. This jamming waveform, characterized by two equal-power tones with a normalized angular frequency separation Δ_{21}^\dagger of $9/(L+1)$ or $2\pi - 9/(L+1)$, jointly maximizes the BMSE of the individual tone estimates and the correlation of estimation errors. This analytical result is then generalized to the K -tone case and refined by introducing an additional frequency correction term per tone, which further optimizes the correlation of estimation errors between non-adjacent tones. Additionally, this paper shows that a jammer composed of equal-power tones, whose normalized angular frequencies are equally spaced by $2\pi/K$, becomes optimal when $K \geq L/2+1$ tones. Overall, this work highlights that the filter length L is a critical parameter from a security perspective. If this parameter is known, low-complexity narrow-band devices can be employed to render the Wiener interpolation filter used in wideband systems completely ineffective.

APPENDIX

A. Derivation of the analytical form of the Wiener interpolation filter \mathbf{w}^* for a multi-tone jammer in DSSS systems

From (4), (9) and (10), the general form of the Wiener filter is $\mathbf{w}^* = \mathbf{C}_{\mathbf{rr}}^{-1}(\boldsymbol{\alpha}, \omega) \mathbf{C}_{\mathbf{r}\boldsymbol{\theta}}(\boldsymbol{\alpha}, \omega) \mathbf{1}_K$. To obtain the special form of the Wiener interpolation filter for a multi-tone jammer in DSSS systems, the matrices $\mathbf{C}_{\mathbf{rr}}(\boldsymbol{\alpha}, \omega)$ and $\mathbf{C}_{\mathbf{r}\boldsymbol{\theta}}(\boldsymbol{\alpha}, \omega)$ are respectively derived in Appendices A1 and A2.

1) *Derivation of the matrix $\mathbf{C}_{\mathbf{rr}}(\boldsymbol{\alpha}, \omega)$* : Firstly, it is noticed that $\mathbf{r}_m(\boldsymbol{\alpha}, \omega) \in \mathbb{C}^K$ is composed of random variables $\mathbf{s}_m \in \mathbb{C}^K$, $\mathbf{n}_m \in \mathbb{C}^K$ and $\mathbf{i}_m(\boldsymbol{\alpha}, \omega) \in \mathbb{C}^K$ that are mutually uncorrelated. Additionally, \mathbf{s}_m and \mathbf{n}_m are independent and identically distributed. Consequently,

$$\begin{aligned} \mathbf{C}_{\mathbf{rr}}(\boldsymbol{\alpha}, \omega) &= \mathbb{E}_{s, n, \phi} [\mathbf{r}_m(\boldsymbol{\alpha}, \omega) \mathbf{r}_m^H(\boldsymbol{\alpha}, \omega)], \\ &= \mathbb{E}_s [\mathbf{s}_m \mathbf{s}_m^H] + \mathbb{E}_n [\mathbf{n}_m \mathbf{n}_m^H] + \mathbb{E}_\phi [\mathbf{i}_m(\boldsymbol{\alpha}, \omega) \mathbf{i}_m^H(\boldsymbol{\alpha}, \omega)], \\ &= (S + \sigma_n^2) \times \mathbf{I}_L + \mathbb{E}_\phi [\mathbf{i}_m(\boldsymbol{\alpha}, \omega) \mathbf{i}_m^H(\boldsymbol{\alpha}, \omega)]. \end{aligned} \quad (\text{A.1})$$

From (1) and (2), it is remarked that $\mathbf{i}_m(\boldsymbol{\alpha}, \omega)$ can be written,

$$\mathbf{i}_m(\boldsymbol{\alpha}, \omega) = \boldsymbol{\Psi}_m(\omega) \boldsymbol{\beta}(\boldsymbol{\alpha}), \quad (\text{A.2})$$

where,

$$\boldsymbol{\Psi}_m(\omega) = [\psi_m(\omega_1), \psi_m(\omega_2), \dots, \psi_m(\omega_K)] \in \mathbb{C}^{L \times K}, \quad (\text{A.3})$$

$$\psi_m(\omega_k) = \left[e^{j(m+\frac{L}{2})\omega_k}, \dots, e^{j(m+1)\omega_k}, e^{j(m-1)\omega_k}, \dots, e^{j(m-\frac{L}{2})\omega_k} \right]^T \in \mathbb{C}^L, \quad (\text{A.4})$$

$$\boldsymbol{\beta}(\boldsymbol{\alpha}) = [\alpha_1 e^{j\phi_1}, \alpha_2 e^{j\phi_2}, \dots, \alpha_K e^{j\phi_K}]^T \in \mathbb{C}^K. \quad (\text{A.5})$$

Therefore, the term $\mathbb{E}_\phi [\mathbf{i}_m \mathbf{i}_m^H]$ can be expressed,

$$\begin{aligned} \mathbb{E}_\phi [\mathbf{i}_m \mathbf{i}_m^H] &= \boldsymbol{\Psi}_m(\omega) \mathbb{E}_\phi [\boldsymbol{\beta}(\boldsymbol{\alpha}) \boldsymbol{\beta}^H(\boldsymbol{\alpha})] \boldsymbol{\Psi}_m^H(\omega), \\ &= \boldsymbol{\Psi}_m(\omega) \mathbf{J}(\boldsymbol{\alpha}) \boldsymbol{\Psi}_m^H(\omega), \\ &= \boldsymbol{\Psi}(\omega) \mathbf{J}(\boldsymbol{\alpha}) \boldsymbol{\Psi}^H(\omega) \end{aligned} \quad (\text{A.6})$$

where $\mathbf{J}(\boldsymbol{\alpha})$ and $\boldsymbol{\Psi}(\omega)$ are given by (14)-(16). Finally, the analytical expression of $\mathbf{C}_{\mathbf{rr}}(\boldsymbol{\alpha}, \omega)$ is obtained by substituting (A.6) into (A.1), yielding (12).

2) *Derivation of the matrix $\mathbf{C}_{\mathbf{r}\boldsymbol{\theta}}(\boldsymbol{\alpha}, \omega)$* : From (2), (A.2) and the mutual uncorrelatedness of \mathbf{s}_m , \mathbf{n}_m and $\mathbf{i}_m(\boldsymbol{\alpha}, \omega)$,

$$\begin{aligned} \mathbf{C}_{\mathbf{r}\boldsymbol{\theta}}(\boldsymbol{\alpha}, \omega) &= \mathbb{E}_{s, n, \phi} [\mathbf{r}_m(\boldsymbol{\alpha}, \omega) \boldsymbol{\theta}_m^H(\boldsymbol{\alpha}, \omega)], \\ &= \mathbb{E}_\phi [\mathbf{i}_m(\boldsymbol{\alpha}, \omega) \boldsymbol{\theta}_m^H(\boldsymbol{\alpha}, \omega)], \\ &= \mathbb{E}_\phi [\boldsymbol{\Psi}_m(\omega) \boldsymbol{\beta}(\boldsymbol{\alpha}) \boldsymbol{\theta}_m^H(\boldsymbol{\alpha}, \omega)], \\ &= \boldsymbol{\Psi}_m(\omega) \text{diag}(\alpha_1^2 e^{-j\omega_1 m}, \dots, \alpha_K^2 e^{-j\omega_K m}), \\ &= \boldsymbol{\Psi}(\omega) \mathbf{J}(\boldsymbol{\alpha}), \end{aligned} \quad (\text{A.7})$$

which concludes the analytical derivation of $\mathbf{C}_{\mathbf{r}\boldsymbol{\theta}}(\boldsymbol{\alpha}, \omega)$ (13) and the proof of Theorem 1.

B. Derivation of the analytical BMSE of the interference estimate $\hat{i}^*(\boldsymbol{\alpha}, \omega)$ for a multi-tone jammer in DSSS systems

From the general expression of the BMSE (8) and the expressions of $i_m(\boldsymbol{\alpha}, \omega)$ and $\hat{i}_m^*(\boldsymbol{\alpha}, \omega)$, respectively given in (1) and (9), the BMSE of the interference estimate $\hat{i}^*(\boldsymbol{\alpha}, \omega)$ can be expressed as,

$$\begin{aligned} \text{BMSE}(\hat{i}^*(\boldsymbol{\alpha}, \omega)) &= \mathbb{E}_{s, n, \phi} [|i_m(\boldsymbol{\alpha}, \omega) - \hat{i}_m^*(\boldsymbol{\alpha}, \omega)|^2], \\ &= \mathbb{E}_{s, n, \phi} \left[\left| \mathbf{1}_K^T \boldsymbol{\epsilon}(\boldsymbol{\alpha}, \omega) \right|^2 \right], \\ &= \mathbf{1}_K^T \mathbf{C}_\epsilon^*(\boldsymbol{\alpha}, \omega) \mathbf{1}_K, \end{aligned} \quad (\text{B.1})$$

where $\boldsymbol{\epsilon}(\boldsymbol{\alpha}, \omega) = \boldsymbol{\theta}_m(\boldsymbol{\alpha}, \omega) - \hat{\boldsymbol{\theta}}_m^*(\boldsymbol{\alpha}, \omega)$ denotes the estimation error between each tone contribution $\boldsymbol{\theta}_m(\boldsymbol{\alpha}, \omega)$ and its estimate $\hat{\boldsymbol{\theta}}_m^*(\boldsymbol{\alpha}, \omega)$, while $\mathbf{C}_\epsilon^*(\boldsymbol{\alpha}, \omega)$ characterizes the minimum error covariance matrix. The latter can be written [25, eq.(12.21)],

$$\begin{aligned} \mathbf{C}_\epsilon^*(\boldsymbol{\alpha}, \omega) &= \mathbb{E}_{s, n, \phi} [\boldsymbol{\epsilon}(\boldsymbol{\alpha}, \omega) \boldsymbol{\epsilon}^H(\boldsymbol{\alpha}, \omega)], \\ &= \mathbf{C}_{\boldsymbol{\theta}\boldsymbol{\theta}}(\boldsymbol{\alpha}, \omega) - \mathbf{C}_{\mathbf{r}\boldsymbol{\theta}}^H(\boldsymbol{\alpha}, \omega) \mathbf{C}_{\mathbf{r}\boldsymbol{\theta}}^{-1}(\boldsymbol{\alpha}, \omega) \mathbf{C}_{\mathbf{r}\boldsymbol{\theta}}(\boldsymbol{\alpha}, \omega), \end{aligned} \quad (\text{B.2})$$

where the covariance matrix $\mathbf{C}_{\boldsymbol{\theta}\boldsymbol{\theta}}(\boldsymbol{\alpha}, \omega)$ reduces to,

$$\begin{aligned} \mathbf{C}_{\boldsymbol{\theta}\boldsymbol{\theta}}(\boldsymbol{\alpha}, \omega) &= \mathbb{E}_\phi [\boldsymbol{\theta}_m(\boldsymbol{\alpha}, \omega) \boldsymbol{\theta}_m^H(\boldsymbol{\alpha}, \omega)], \\ &= \mathbf{J}(\boldsymbol{\alpha}). \end{aligned} \quad (\text{B.3})$$

Consequently, from (B.2), (B.3), (12) and (13),

$$\begin{aligned} \mathbf{C}_\epsilon^*(\boldsymbol{\alpha}, \omega) &= \mathbf{J}(\boldsymbol{\alpha}) - \mathbf{J}(\boldsymbol{\alpha}) \boldsymbol{\Psi}^H(\omega) \times \\ &\quad \left((S + \sigma_n^2) \mathbf{I}_L + \boldsymbol{\Psi}(\omega) \mathbf{J}(\boldsymbol{\alpha}) \boldsymbol{\Psi}^H(\omega) \right)^{-1} \boldsymbol{\Psi}(\omega) \mathbf{J}(\boldsymbol{\alpha}). \end{aligned} \quad (\text{B.4})$$

To further simplify this equation, the matrix \mathbf{B} is first defined by setting $\mathbf{B} = \mathbf{J}^{-1}(\boldsymbol{\alpha}) + (S + \sigma_n^2)^{-1} \boldsymbol{\Gamma}(\omega)$, where

$\Gamma(\omega) = \Psi^H(\omega)\Psi(\omega)$. It's worth noting that $[\Gamma(\omega)]_{kk'}$ allows a closed-form expression given by,

$$\begin{aligned} [\Gamma(\omega)]_{kk'} &= \psi^H(\omega_k)\psi(\omega_{k'}), \\ &= \sum_{\substack{l=-L/2 \\ l \neq 0}}^{L/2} e^{jl(\omega_{k'} - \omega_k)}, \\ &= \frac{\sin\left(\frac{L+1}{2}\Delta_{k'k}\right)}{\sin\left(\frac{1}{2}\Delta_{k'k}\right)} - 1, \\ &= D_{L/2}(\Delta_{k'k}) - 1, \end{aligned} \quad (\text{B.5})$$

where $\Delta_{k'k} = \omega_{k'} - \omega_k$ is the normalized angular frequency difference between the k' th tone and the k th one, and $D_n(x) = \sin((n+1/2)x)/\sin(x/2)$ denotes the n th Dirichlet kernel. After using the Woodbury identity, the matrix $\mathbf{C}_\epsilon^*(\alpha, \omega)$ reduces to,

$$\begin{aligned} \mathbf{C}_\epsilon^*(\alpha, \omega) &= \mathbf{J}(\alpha) - \mathbf{J}(\alpha)\Psi^H(\omega) \times \\ &\quad \left[(S + \sigma_n^2)^{-1}\mathbf{I}_L - (S + \sigma_n^2)^{-2}\Psi(\omega)\mathbf{B}^{-1}\Psi^H(\omega) \right] \Psi(\omega)\mathbf{J}(\alpha), \\ &= \mathbf{J}(\alpha) - \mathbf{J}(\alpha) \left[(\mathbf{B} - \mathbf{J}^{-1}(\alpha)) - \right. \\ &\quad \left. (\mathbf{B} - \mathbf{J}^{-1}(\alpha))\mathbf{B}^{-1}(\mathbf{B} - \mathbf{J}^{-1}(\alpha)) \right] \mathbf{J}(\alpha), \\ &= \mathbf{B}^{-1}. \end{aligned} \quad (\text{B.6})$$

Finally, (18) and (19) are obtained by substituting (B.6) into (B.1), which concludes the proof of Theorem 2.

C. Closed-form derivation of the partial derivatives of $\mathcal{L}(\alpha, \omega, \lambda)$

This section details the closed-form derivation of $\partial\mathcal{L}(\alpha, \omega, \lambda)/\partial\alpha_k^2$ in Appendix C1 and $\partial\mathcal{L}(\alpha, \omega, \lambda)/\partial\omega_k$ in Appendix C2.

1) *Derivation of $\partial\mathcal{L}(\alpha, \omega, \lambda)/\partial\alpha_k^2$:* From the differential properties $d(\mathbf{XY}) = d(\mathbf{X})\mathbf{Y} + \mathbf{X}d(\mathbf{Y})$ and $d\mathbf{X}^{-1} = -\mathbf{X}^{-1}(d\mathbf{X})\mathbf{X}^{-1}$, the partial derivatives of \mathbf{XY} and \mathbf{X}^{-1} with respect to α_k^2 are respectively written [31],

$$\frac{\partial(\mathbf{XY})}{\partial\alpha_k^2} = \frac{\partial\mathbf{X}}{\partial\alpha_k^2}\mathbf{Y} + \mathbf{X}\frac{\partial\mathbf{Y}}{\partial\alpha_k^2}, \quad (\text{C.1})$$

$$\frac{\partial(\mathbf{X}^{-1})}{\partial\alpha_k^2} = -\mathbf{X}^{-1}\frac{\partial\mathbf{X}}{\partial\alpha_k^2}\mathbf{X}^{-1}. \quad (\text{C.2})$$

Therefore, from (17), (18) and (C.1), the partial derivative of $\mathcal{L}(\alpha, \omega, \lambda)$ with respect to α_k^2 is written,

$$\begin{aligned} \frac{\partial\mathcal{L}(\alpha, \omega, \lambda)}{\partial\alpha_k^2} &= -\mathbf{1}_K^T \left(\frac{\partial\mathbf{A}^{-1}(\alpha, \omega)}{\partial\alpha_k^2} \mathbf{J}(\alpha) + \right. \\ &\quad \left. \mathbf{A}^{-1}(\alpha, \omega) \frac{\partial\mathbf{J}(\alpha)}{\partial\alpha_k^2} \right) \mathbf{1}_K + \lambda, \end{aligned} \quad (\text{C.3})$$

where,

$$\frac{\partial\mathbf{J}(\alpha)}{\partial\alpha_k^2} = \text{diag}(0, \dots, 0, \underbrace{1}_{\substack{k^{\text{th}} \\ \text{element}}}, 0, \dots, 0). \quad (\text{C.4})$$

Additionally, using property (C.2), the term $\partial\mathbf{A}^{-1}(\alpha, \omega)/\partial\alpha_k^2$ is expressed as,

$$\begin{aligned} \frac{\partial\mathbf{A}^{-1}(\alpha, \omega)}{\partial\alpha_k^2} &= -\mathbf{A}^{-1}(\alpha, \omega) \frac{\partial\mathbf{A}(\alpha, \omega)}{\partial\alpha_k^2} \mathbf{A}^{-1}(\alpha, \omega), \\ &= -(S + \sigma_n^2)^{-1} \mathbf{A}^{-1}(\alpha, \omega) \frac{\partial\mathbf{J}(\alpha)}{\partial\alpha_k^2} \mathbf{A}^{-1}(\alpha, \omega). \end{aligned} \quad (\text{C.5})$$

Then, by substituting (C.5) into (C.3) and exploiting the matrix inverse property given in [32, eq.(166)],

$$\frac{\partial\mathcal{L}(\alpha, \omega, \lambda)}{\partial\alpha_k^2} = -\mathbf{1}_K^T \mathbf{A}^{-1}(\alpha, \omega) \frac{\partial\mathbf{J}(\alpha)}{\partial\alpha_k^2} \times \quad (\text{C.6})$$

$$\begin{aligned} &\left(\mathbf{I}_K - \frac{\Gamma(\omega)}{S + \sigma_n^2} \left(\mathbf{I}_K + \mathbf{J}(\alpha) \frac{\Gamma(\omega)}{S + \sigma_n^2} \right)^{-1} \mathbf{J}(\alpha) \right) \mathbf{1}_K + \lambda, \\ &= -\mathbf{1}_K^T \mathbf{A}^{-1}(\alpha, \omega) \frac{\partial\mathbf{J}(\alpha)}{\partial\alpha_k^2} \left(\mathbf{I}_K + \frac{\Gamma(\omega)}{S + \sigma_n^2} \mathbf{J}(\alpha) \right)^{-1} \mathbf{1}_K + \lambda, \\ &= -\mathbf{1}_K^T \mathbf{A}^{-1}(\alpha, \omega) \frac{\partial\mathbf{J}(\alpha)}{\partial\alpha_k^2} \mathbf{A}^{-T}(\alpha, \omega) \mathbf{1}_K + \lambda, \end{aligned} \quad (\text{C.7})$$

which results in (28) and (29) by substituting (C.4) into (C.6).

2) *Derivation of $\partial\mathcal{L}(\alpha, \omega, \lambda)/\partial\omega_k$:* From (17), (18) and (C.1), the partial derivative of $\mathcal{L}(\alpha, \omega, \lambda)$ with respect to ω_k is written,

$$\begin{aligned} \frac{\partial\mathcal{L}(\alpha, \omega, \lambda)}{\partial\omega_k} &= -\mathbf{1}_K^T \frac{\partial(\mathbf{A}^{-1}(\alpha, \omega)\mathbf{J}(\alpha))}{\partial\omega_k} \mathbf{1}_K, \\ &= -\mathbf{1}_K^T \frac{\partial\mathbf{A}^{-1}(\alpha, \omega)}{\partial\omega_k} \mathbf{J}(\alpha) \mathbf{1}_K. \end{aligned} \quad (\text{C.8})$$

Using (C.2), $\partial\mathbf{A}^{-1}(\alpha, \omega)/\partial\omega_k$ can be written as,

$$\frac{\partial\mathbf{A}^{-1}(\alpha, \omega)}{\partial\omega_k} = -\frac{\mathbf{A}^{-1}(\alpha, \omega)}{S + \sigma_n^2} \mathbf{J}(\alpha) \frac{\partial\Gamma(\omega)}{\partial\omega_k} \mathbf{A}^{-1}(\alpha, \omega), \quad (\text{C.9})$$

where $\partial\Gamma(\omega)/\partial\omega_k$ is expressed as,

$$\begin{aligned} \frac{\partial\Gamma(\omega)}{\partial\omega_k} &= \frac{\partial}{\partial\omega_k} \begin{bmatrix} L & \Gamma_{12} & \dots & \Gamma_{1k} & \dots & \Gamma_{1K} \\ \Gamma_{21} & L & \dots & \Gamma_{2k} & \dots & \Gamma_{2K} \\ \vdots & \vdots & \ddots & \vdots & \dots & \vdots \\ \Gamma_{k1} & \Gamma_{k2} & \dots & L & \dots & \Gamma_{kK} \\ \vdots & \vdots & & \vdots & \ddots & \vdots \\ \Gamma_{K1} & \Gamma_{K2} & \dots & \Gamma_{Kk} & \dots & L \end{bmatrix}, \\ &= \begin{bmatrix} 0 & 0 & \dots & \frac{\partial\Gamma_{1k}}{\partial\omega_k} & \dots & 0 \\ 0 & 0 & \dots & \frac{\partial\Gamma_{2k}}{\partial\omega_k} & \dots & 0 \\ \vdots & \vdots & \ddots & \vdots & \dots & \vdots \\ \frac{\partial\Gamma_{k1}}{\partial\omega_k} & \frac{\partial\Gamma_{k2}}{\partial\omega_k} & \dots & 0 & \dots & \frac{\partial\Gamma_{kk}}{\partial\omega_k} \\ \vdots & \vdots & & \vdots & \ddots & \vdots \\ 0 & 0 & \dots & \frac{\partial\Gamma_{Kk}}{\partial\omega_k} & \dots & 0 \end{bmatrix}. \end{aligned} \quad (\text{C.10})$$

In this matrix, elements $\left[\frac{\partial\Gamma(\omega)}{\partial\omega_k}\right]_{kk'}$ and $\left[\frac{\partial\Gamma(\omega)}{\partial\omega_k}\right]_{k'k}$ are derived from (21) to give (31) and (32). Finally, (C.9) is substituted into (C.8) to obtain (30), ending the proof of Theorem 3.

D. Optimization of a 2-tone jammer

In this section, the closed-form expression of the optimal 2-tone jammer is derived. To this end, the optimal solution α^\dagger is first established in Appendix D1, before deriving the optimal solution ω^\dagger in Appendix D2.

1) *Proof that $\alpha^\dagger = [\sqrt{J/2}, \sqrt{J/2}]^T$* : First, the convexity of the Lagrangian function $\mathcal{L}(\alpha, \omega, \lambda)$ with respect to $\alpha_k^2 > 0$ is examined, treating ω as a fixed parameter. From (19), (29) and the formula of the inverse for a 2×2 matrix, coefficients $e_{kk'} = [\mathbf{E}(\alpha, \omega)]_{kk'}$ are given by,

$$\left\{ \begin{array}{l} e_{11} = \nu(\alpha_1^2, \alpha_2^2) \times (1 + \alpha_2^2 L / (S + \sigma_n^2)) \\ e_{22} = \nu(\alpha_1^2, \alpha_2^2) \times (1 + \alpha_1^2 L / (S + \sigma_n^2)) \\ e_{21} = -\nu(\alpha_1^2, \alpha_2^2) \times \alpha_2^2 (D_{L/2}(\Delta_{21}) - 1) / (S + \sigma_n^2) \\ e_{12} = -\nu(\alpha_1^2, \alpha_2^2) \times \alpha_1^2 (D_{L/2}(\Delta_{21}) - 1) / (S + \sigma_n^2) \\ \nu(\alpha_1^2, \alpha_2^2) = [1 + (\alpha_1^2 + \alpha_2^2) L / (S + \sigma_n^2) + \alpha_1^2 \alpha_2^2 \times [L^2 - (D_{L/2}(\Delta_{21}) - 1)^2] / (S + \sigma_n^2)^2]^{-1} \end{array} \right. . \quad (\text{D.1})$$

Partial derivatives of $\mathcal{L}(\alpha, \omega, \lambda)$ with respect to α_k^2 are then calculated from (28) and become,

$$\left\{ \begin{array}{l} \frac{\partial \mathcal{L}(\alpha, \omega, \lambda)}{\partial \alpha_1^2} = -[\nu(\alpha_1^2, \alpha_2^2)]^2 \times \left[1 + \alpha_2^2 \frac{\gamma}{S + \sigma_n^2}\right]^2 + \lambda \\ \frac{\partial \mathcal{L}(\alpha, \omega, \lambda)}{\partial \alpha_2^2} = -[\nu(\alpha_1^2, \alpha_2^2)]^2 \times \left[1 + \alpha_1^2 \frac{\gamma}{S + \sigma_n^2}\right]^2 + \lambda \end{array} \right. , \quad (\text{D.2})$$

where $\gamma = L - (D_{L/2}(\Delta_{21}) - 1) \geq 0$. Recalling that the Lagrangian function $\mathcal{L}(\alpha, \omega, \lambda)$ is convex with respect to α_k^2 if and only if $\partial \mathcal{L}(\alpha, \omega, \lambda) / \partial \alpha_k^2$ is an increasing function, the monotonicity of (D.2) is studied. From the analytical expression of $\nu(\alpha_1^2, \alpha_2^2)$ (D.1), the function $-\left[\nu(\alpha_1^2, \alpha_2^2)\right]^2$ is an increasing function for $\alpha_1^2 > 0$ (resp. $\alpha_2^2 > 0$). Therefore, $\partial \mathcal{L}(\alpha, \omega, \lambda) / \partial \alpha_1^2$ (resp. $\partial \mathcal{L}(\alpha, \omega, \lambda) / \partial \alpha_2^2$) is also an increasing function over the same interval. As a consequence, $\mathcal{L}(\alpha, \omega, \lambda)$ is convex on $\alpha_1^2 > 0$ and $\alpha_2^2 > 0$. The Lagrangian function is thus minimized when $\partial \mathcal{L}(\alpha, \omega, \lambda) / \partial \alpha_1^2 = \partial \mathcal{L}(\alpha, \omega, \lambda) / \partial \alpha_2^2 = 0$ and $\partial \mathcal{L}(\alpha, \omega, \lambda) / \partial \lambda = 0$, which are obtained for $\alpha_1^2 = \alpha_2^2 = J/2$, leading to the final result (33).

2) *Proof that $\omega^\dagger = [\omega_1, \omega_1 + \Delta_{21}^\dagger]^T$* : First, the convexity of the Lagrangian function $\mathcal{L}(\alpha, \omega, \lambda)$ with respect to ω_k is studied. In particular, this study is led for the optimal amplitude configuration $\alpha^\dagger = [\sqrt{J/2}, \sqrt{J/2}]^T$, for which $\mathbf{J}(\alpha^\dagger) = (J/2)\mathbf{I}_2$. Thus, from (18), (30) and (31), partial derivatives of $\partial \mathcal{L}(\alpha^\dagger, \omega, \lambda^\dagger)$ with respect to ω_k are expressed as,

$$\begin{aligned} \frac{\partial \mathcal{L}(\alpha^\dagger, \omega, \lambda^\dagger)}{\partial \omega_1} &= (S + \sigma_n^2)^{-1} \frac{\partial D_{L/2}(\Delta_{21})}{\partial \omega_1} \mathbf{1}_2^T \begin{bmatrix} c_1 & c_2 \\ c_2 & c_1 \end{bmatrix} \times \\ &\quad \begin{bmatrix} 0 & 1 \\ 1 & 0 \end{bmatrix} \begin{bmatrix} c_1 & c_2 \\ c_2 & c_1 \end{bmatrix} \mathbf{1}_2, \\ &= \frac{2}{S + \sigma_n^2} \frac{\partial D_{L/2}(\Delta_{21})}{\partial \omega_1} (c_1 + c_2)^2, \end{aligned} \quad (\text{D.3})$$

and,

$$\frac{\partial \mathcal{L}(\alpha^\dagger, \omega, \lambda^\dagger)}{\partial \omega_2} = -\frac{2}{S + \sigma_n^2} \frac{\partial D_{L/2}(\Delta_{21})}{\partial \omega_1} (c_1 + c_2)^2, \quad (\text{D.4})$$

with,

$$\left\{ \begin{array}{l} c_1 = \nu(J/2, J/2)(J/2)(1 + (J/2)L / (S + \sigma_n^2)) \\ c_2 = -\nu(J/2, J/2)(J/2)^2 (D_{L/2}(\Delta_{21}) - 1) / (S + \sigma_n^2) \\ \nu(J/2, J/2) = [1 + (J/2)\gamma / (S + \sigma_n^2)]^{-1} \times \\ \quad [1 + (J/2)(L + D_{L/2}(\Delta_{21}) - 1) / (S + \sigma_n^2)]^{-1} \end{array} \right. . \quad (\text{D.5})$$

From (32), (D.3) and (D.4), $\partial \mathcal{L}(\alpha^\dagger, \omega, \lambda^\dagger) / \partial \omega_1$ (resp. $\partial \mathcal{L}(\alpha^\dagger, \omega, \lambda^\dagger) / \partial \omega_2$) is a non-monotonic function with respect to ω_1 (resp. ω_2) and $\mathcal{L}(\alpha^\dagger, \omega, \lambda^\dagger)$ is non-convex. In order to find the global minima of this function, its analytical form is first derived from (17) and (D.5),

$$\begin{aligned} \mathcal{L}(\alpha^\dagger, \omega, \lambda^\dagger) &= -J\nu(J/2, J/2) [1 + (J/2)\gamma / (S + \sigma_n^2)], \\ &= -(S + \sigma_n^2) \left[\frac{S + \sigma_n^2}{J} + \frac{L - 1}{2} + \frac{D_{L/2}(\Delta_{21})}{2} \right]^{-1}. \end{aligned} \quad (\text{D.6})$$

Therefore, the Lagrangian function $\mathcal{L}(\alpha^\dagger, \omega, \lambda^\dagger)$ is minimized for the Δ_{21}^\dagger value such that,

$$\Delta_{21}^\dagger = \arg \min_{\Delta_{21}} (D_{L/2}(\Delta_{21})). \quad (\text{D.7})$$

A rough approximate solution to this problem is first found. By noticing that $D_{L/2}(\Delta_{21})$ is the product of $\sin(\frac{L+1}{2}\Delta_{21})$ and $1 / \sin(\frac{1}{2}\Delta_{21})$, the latter being a decreasing function of $\Delta_{21} \in]0, \pi]$, the solution to (D.7) can be approximated by the smallest value Δ_{21} that minimizes $\sin(\frac{L+1}{2}\Delta_{21})$. This first solution, denoted $\Delta_{21}^{\dagger(1)}$, is expressed as,

$$\Delta_{21}^{\dagger(1)} = 3\pi / (L + 1), \quad (\text{D.8})$$

and is depicted in Figure 6a with the optimal solution Δ_{21}^\dagger . From (D.8), it is clear that the more L increases, the smaller $\Delta_{21}^{\dagger(1)}$ is. From this observation, the function $1 / \sin(\Delta_{21}/2)$ can be accurately approximated by its Taylor expansion $2/\Delta_{21} + o(1/\Delta_{21})$. Therefore, the problem (D.7) is rewritten,

$$\Delta_{21}^{\dagger} = \arg \min_{\Delta_{21}} (\tilde{D}_{L/2}(\Delta_{21})), \quad (\text{D.9})$$

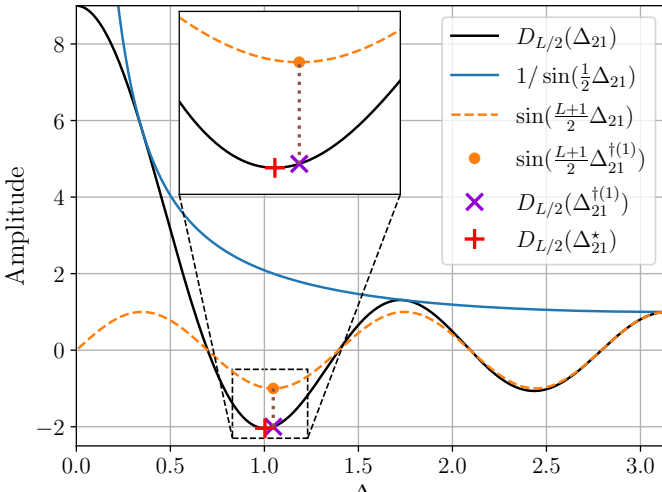
where,

$$\tilde{D}_{L/2}(\Delta_{21}) = (L + 1) \times \text{sinc}(x), \quad (\text{D.10})$$

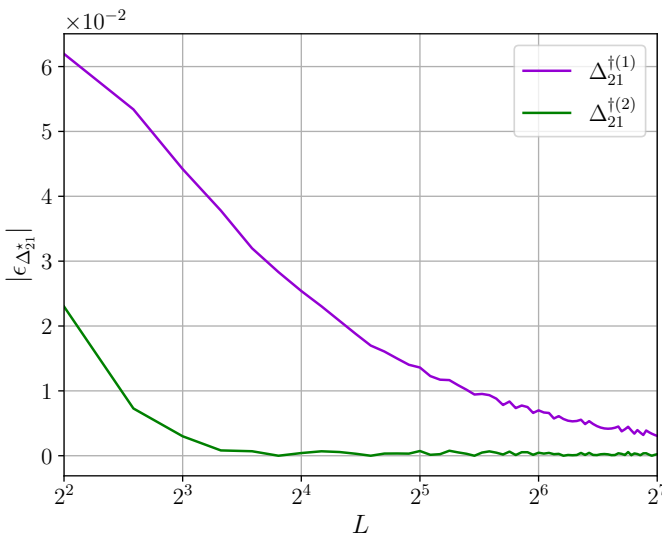
with $\text{sinc}(x) = \sin(x)/x$ and $x = \frac{L+1}{2} \times \Delta_{21}$, is a good approximate of $D_{L/2}(\Delta_{21})$ for high L values. By the same reasoning as for $\Delta_{21}^{\dagger(1)}$, the solution to (D.9) is obtained for the smallest value Δ_{21} , denoted $\Delta_{21}^{\dagger(2)}$, such that $\partial \tilde{D}_{L/2}(\Delta_{21}) / \partial \omega_1 = 0$. Thus, the partial derivative of $\tilde{D}_{L/2}(\Delta_{21})$ with respect to ω_1 is first determined,

$$\frac{\partial \tilde{D}_{L/2}(\Delta_{21})}{\partial \omega_1} = \frac{-\frac{L+1}{2} \cos(\frac{L+1}{2}\Delta_{21}) + \sin(\frac{L+1}{2}\Delta_{21})}{\Delta_{21}^2}. \quad (\text{D.11})$$

By equating this partial derivative to 0, the equation to solve takes the form $x = \tan(x)$. The first solution to equation $x = \tan(x)$, which is the solution of interest as previously explained, is approximated by $x = 4.493$ [33][eq.(34:7:6)].



(a) $\Delta_{21}^{(1)}$ approximate solution.



(b) Absolute difference $\epsilon_{\Delta_{21}^*}$ with respect to the filter length L

Fig. 6: Optimal solution for the 2-tone jamming waveform

Consequently, the second approximate solution to problem (D.7) is written,

$$\Delta_{21}^{(2)} = 9/(L+1). \quad (\text{D.12})$$

In order to choose the best approximation, the absolute difference $\epsilon_{\Delta_{21}^*} = |\Delta_{21}^* - \Delta_{21}^{(X)}|$ is calculated and depicted in Figure 6 for L ranging from 4 to 128. It is observed that both solutions converge to the optimal solution and that a faster convergence is obtained for $\Delta_{21}^{(2)}$. Consequently, $\Delta_{21}^{(2)}$ is preferred to $\Delta_{21}^{(1)}$. Finally, reminding that the Dirichlet kernel is an even 2π -periodic function, the expressions (34) and (35) are obtained, ending the proof of Proposition 1.

E. BMSE calculation for the optimal jammer composed of $K = (L/2) + 1$ tones

In this section, the analytical expression of the BMSE is determined for the jamming configuration $\{\alpha^\ddagger, \omega^\ddagger\}$ characterized by (45) and (46). For this configuration, it is first observed that $[\Gamma(\omega)]_{(k+1)(k'+1)} = [\Gamma(\omega)]_{kk'} = [\Gamma(\omega)]_{(k+1)1}$. Therefore, $\Gamma(\omega)$ is a circulant matrix that can be diagonalized in such a manner that $\Gamma(\omega) = \mathbf{U}\Lambda\mathbf{U}^H$, where \mathbf{U} is an IDFT matrix and Λ is a diagonal matrix composed of the eigenvalues $\lambda_i = \sum_{k'=1}^K [\Gamma(\omega)]_{1k'} \times \omega^{(i-1)(k'-1)}$, with $i \in \{1, \dots, K\}$ and $\omega = e^{j\frac{2\pi}{K}}$. From (17) the BMSE of the interference estimate $\hat{i}^*(\alpha^\ddagger, \omega^\ddagger)$ is then written,

$$\begin{aligned} \text{BMSE} \left(\hat{i}^*(\alpha^\ddagger, \omega^\ddagger) \right) &= \mathbf{1}_K^T \left(\frac{K}{J} \mathbf{I}_K + \frac{\mathbf{U}\Lambda\mathbf{U}^H}{S + \sigma_n^2} \right)^{-1} \mathbf{1}_K, \\ &= \mathbf{1}_K^T \mathbf{U} \left(\frac{K}{J} \mathbf{I}_K + \frac{\Lambda}{S + \sigma_n^2} \right)^{-1} \mathbf{U}^H \mathbf{1}_K, \\ &= K [1, 0, \dots, 0] \text{diag}(\zeta_1, \dots, \zeta_K) [1, 0, \dots, 0]^T, \\ &= K \zeta_1, \end{aligned} \quad (\text{E.1})$$

where $\zeta_k = (K/J + \lambda_k/(S + \sigma_n^2))^{-1}$. Therefore, the BMSE highly depends on the eigenvalue λ_1 , which is expressed as,

$$\begin{aligned} \lambda_1 &= \sum_{k'=1}^K [\Gamma(\omega)]_{1k'}, \\ &= L - K + 1 + \sum_{k'=2}^K D_{L/2} \left(\frac{2\pi}{K} (k' - 1) \right), \\ &= L - K + 1 + \sum_{l=-L/2}^{L/2} \sum_{k'=2}^K e^{jl\frac{2\pi}{K}(k'-1)}, \\ &= L + \sum_{\substack{l=-L/2 \\ l \neq 0}}^{L/2} f(l), \end{aligned} \quad (\text{E.2})$$

where,

$$f(l) = \frac{\cos(l\pi) \sin(l\pi(K-1)/K)}{\sin(l\pi/K)}. \quad (\text{E.3})$$

It can be shown that the function $f(l)$ admits two values. For l values such that $l = nK$, with $n \in \mathbb{N}^*$, l'Hôpital's rule is used to obtain $f(l) = K - 1$. The number of values l that respect this condition is equal to $2 \lfloor \frac{L}{2K} \rfloor$. For other values of l , $f(l) = -1$ is obtained from (E.3) using the angle sum identity. Consequently, λ_1 simplifies to,

$$\begin{aligned} \lambda_1 &= L + (K-1) \times 2 \left\lfloor \frac{L}{2K} \right\rfloor - 1 \times \left(L - 2 \left\lfloor \frac{L}{2K} \right\rfloor \right), \\ &= 2K \left\lfloor \frac{L}{2K} \right\rfloor. \end{aligned} \quad (\text{E.4})$$

Substituting (E.4) into (E.1), (47) is obtained, ending the proof of Proposition 2.

REFERENCES

- [1] Y. Liu, H.-H. Chen, and L. Wang, "Physical Layer Security for Next Generation Wireless Networks: Theories, Technologies, and Challenges," *IEEE Communications Surveys & Tutorials*, vol. 19, no. 1, pp. 347–376, 2017. [Online]. Available: <http://ieeexplore.ieee.org/document/7539590/>
- [2] P. Yue, J. An, J. Zhang, J. Ye, G. Pan, S. Wang, P. Xiao, and L. Hanzo, "Low Earth Orbit Satellite Security and Reliability: Issues, Solutions, and the Road Ahead," *IEEE Communications Surveys & Tutorials*, vol. 25, no. 3, pp. 1604–1652, 2023. [Online]. Available: <https://ieeexplore.ieee.org/document/10209551/>
- [3] A. Tusha and H. Arslan, "Interference Burden in Wireless Communications: A Comprehensive Survey From PHY Layer Perspective," *IEEE Communications Surveys & Tutorials*, vol. 27, no. 4, pp. 2204–2246, Aug. 2025. [Online]. Available: <https://ieeexplore.ieee.org/document/10736552/>
- [4] R. Morales-Ferre, P. Richter, E. Falletti, A. De La Fuente, and E. S. Lohan, "A Survey on Coping With Intentional Interference in Satellite Navigation for Manned and Unmanned Aircraft," *IEEE Communications Surveys & Tutorials*, vol. 22, no. 1, pp. 249–291, 2020. [Online]. Available: <https://ieeexplore.ieee.org/document/8882350/>
- [5] C. Hegarty, A. J. Van Dierendonck, D. Bobyn, M. Tran, and J. Grabowski, "Suppression of Pulsed Interference through Blanking," Jun. 2000, pp. 399–408.
- [6] D. Borio, C. O'Driscoll, and J. Fortuny, "GNSS Jammers: Effects and countermeasures," in *2012 6th ESA Workshop on Satellite Navigation Technologies (Navitec 2012) & European Workshop on GNSS Signals and Signal Processing*, Dec. 2012, pp. 1–7, iSSN: 2325-5455. [Online]. Available: <https://ieeexplore.ieee.org/document/6423048/>
- [7] D. Borio, "Swept GNSS jamming mitigation through pulse blanking," in *2016 European Navigation Conference (ENC)*, Helsinki, Finland: IEEE, May 2016, pp. 1–8. [Online]. Available: <http://ieeexplore.ieee.org/document/7530549/>
- [8] M. Aygur, S. Kanadeepan, A. Giorgetti, A. Al-Hourani, E. Arbon, and M. Bowyer, "Narrowband Interference Mitigation Techniques: A Survey," *IEEE Communications Surveys & Tutorials*, pp. 1–1, 2025. [Online]. Available: <https://ieeexplore.ieee.org/document/10845757/>
- [9] E. Masry, "Closed-Form Analytical Results for the Rejection of Narrow-Band Interference in PN Spread-Spectrum Systems—Part I: Linear Prediction Filters," *IEEE Transactions on Communications*, vol. 32, no. 8, pp. 888–896, Aug. 1984. [Online]. Available: <http://ieeexplore.ieee.org/document/1096164/>
- [10] Y.-C. Wang and L. Milstein, "Rejection of multiple narrow-band interference in both BPSK and QPSK DS spread-spectrum systems," *IEEE Transactions on Communications*, vol. 36, no. 2, pp. 195–204, Feb. 1988. [Online]. Available: <https://ieeexplore.ieee.org/document/2750/>
- [11] J. Ketchum and J. Proakis, "Adaptive Algorithms for Estimating and Suppressing Narrow-Band Interference in PN Spread-Spectrum Systems," *IEEE Transactions on Communications*, vol. 30, no. 5, pp. 913–924, May 1982. [Online]. Available: <http://ieeexplore.ieee.org/document/1095542/>
- [12] J. Young and J. Lehnert, "Analysis of DFT-based frequency excision algorithms for direct-sequence spread-spectrum communications," *IEEE Transactions on Communications*, vol. 46, no. 8, pp. 1076–1087, Aug. 1998. [Online]. Available: <http://ieeexplore.ieee.org/document/705409/>
- [13] H. Krim and M. Viberg, "Two decades of array signal processing research: the parametric approach," *IEEE Signal Processing Magazine*, vol. 13, no. 4, pp. 67–94, Jul. 1996. [Online]. Available: <http://ieeexplore.ieee.org/document/526899/>
- [14] W. Myrick, J. Goldstein, and M. Zoltowski, "Low complexity anti-jam space-time processing for GPS," in *2001 IEEE International Conference on Acoustics, Speech, and Signal Processing. Proceedings (Cat. No.01CH37221)*. Salt Lake City, UT, USA: IEEE, 2001, pp. 2233–2236. [Online]. Available: <http://ieeexplore.ieee.org/document/940442/>
- [15] L. Musumeci and F. Dovis, "Use of the Wavelet Transform for Interference Detection and Mitigation in Global Navigation Satellite Systems," *International Journal of Navigation and Observation*, vol. 2014, pp. 1–14, Feb. 2014. [Online]. Available: <https://www.hindawi.com/journals/ijno/2014/262186/>
- [16] Y. Hu, S. Huang, L. Zhao, and M. Jiang, "Narrowband Interference Cancellation for OFDM Based on Deep Learning and Compressed Sensing," *IEEE Transactions on Signal Processing*, vol. 73, pp. 1612–1625, 2025. [Online]. Available: <https://ieeexplore.ieee.org/document/10772564/>
- [17] Y. Huang, G. Liao, Y. Xiang, Z. Zhang, J. Li, and A. Nehorai, "Reweighted Nuclear Norm and Reweighted Frobenius Norm Minimizations for Narrowband RFI Suppression on SAR System," *IEEE Transactions on Geoscience and Remote Sensing*, vol. 57, no. 8, pp. 5949–5962, Aug. 2019. [Online]. Available: <https://ieeexplore.ieee.org/document/8681711/>
- [18] D. Borio, L. Camoriano, and L. Lo Presti, "Two-Pole and Multi-Pole Notch Filters: A Computationally Effective Solution for GNSS Interference Detection and Mitigation," *IEEE Systems Journal*, vol. 2, no. 1, pp. 38–47, Mar. 2008. [Online]. Available: <http://ieeexplore.ieee.org/document/4433998/>
- [19] Y.-R. Chien, "Design of GPS Anti-Jamming Systems Using Adaptive Notch Filters," *IEEE Systems Journal*, vol. 9, no. 2, pp. 451–460, Jun. 2015. [Online]. Available: <https://ieeexplore.ieee.org/document/6631513/>
- [20] E. Masry, "Closed-Form Analytical Results for the Rejection of Narrow-Band Interference in PN Spread-Spectrum Systems—Part II: Linear Interpolation Filters," *IEEE Transactions on Communications*, vol. 33, no. 1, pp. 10–19, Jan. 1985. [Online]. Available: <http://ieeexplore.ieee.org/document/1096204/>
- [21] Loh-Ming Li and L. Milstein, "Rejection of Narrow-Band Interference in PN Spread-Spectrum Systems Using Transversal Filters," *IEEE Transactions on Communications*, vol. 30, no. 5, pp. 925–928, May 1982. [Online]. Available: <http://ieeexplore.ieee.org/document/1095543/>
- [22] R. Iltis and L. Milstein, "Performance Analysis of Narrow-Band Interference Rejection Techniques in DS Spread-Spectrum Systems," *IEEE Transactions on Communications*, vol. 32, no. 11, pp. 1169–1177, Nov. 1984. [Online]. Available: <http://ieeexplore.ieee.org/document/1095986/>
- [23] E. Masry and L. Milstein, "Performance of DS Spread-Spectrum Receiver Employing Interference-Suppression Filters Under a Worst-Case Jamming Condition," *IEEE Transactions on Communications*, vol. 34, no. 1, pp. 13–21, 1986. [Online]. Available: <http://ieeexplore.ieee.org/document/1096425/>
- [24] C. Fonteneau, M. Crussière, A. Bazin, and O. P. Pasquier, "Rejection Capability of Anti-Jamming Wiener Filter for Multi-Tone Interference in DSSS Systems," in *MILCOM 2024 - 2024 IEEE Military Communications Conference (MILCOM)*. Washington, DC, USA: IEEE, Oct. 2024, pp. 1–6. [Online]. Available: <https://ieeexplore.ieee.org/document/10773998/>
- [25] S. M. Kay, *Fundamentals of statistical signal processing: estimation theory*. USA: Prentice-Hall, Inc., 1993.
- [26] J. Goldstein, I. Reed, and L. Scharf, "A multistage representation of the Wiener filter based on orthogonal projections," *IEEE Transactions on Information Theory*, vol. 44, no. 7, pp. 2943–2959, Nov. 1998. [Online]. Available: <http://ieeexplore.ieee.org/document/737524/>
- [27] M. Honig and J. Goldstein, "Adaptive reduced-rank interference suppression based on the multistage Wiener filter," *IEEE Transactions on Communications*, vol. 50, no. 6, pp. 986–994, Jun. 2002. [Online]. Available: <http://ieeexplore.ieee.org/document/1010618/>
- [28] N. Song, R. C. De Lamare, M. Haardt, and M. Wolf, "Adaptive Widely Linear Reduced-Rank Interference Suppression Based on the Multistage Wiener Filter," *IEEE Transactions on Signal Processing*, vol. 60, no. 8, pp. 4003–4016, Aug. 2012. [Online]. Available: <https://ieeexplore.ieee.org/document/6194364/>
- [29] M. Zhang, A. Zhang, and J. Li, "Fast and Accurate Rank Selection Methods for Multistage Wiener Filter," *IEEE Transactions on Signal Processing*, vol. 64, no. 4, pp. 973–984, Feb. 2016. [Online]. Available: <http://ieeexplore.ieee.org/document/7305823/>
- [30] D. P. Kingma and J. Ba, "Adam: A Method for Stochastic Optimization," Jan. 2017, arXiv:1412.6980. [Online]. Available: <http://arxiv.org/abs/1412.6980>
- [31] T. P. Minka, "Old and new matrix algebra useful for statistics," 2000. [Online]. Available: <https://api.semanticscholar.org/CorpusID:15971655>
- [32] K. B. Petersen and M. S. Pedersen, "The matrix cookbook," 2006. [Online]. Available: <https://api.semanticscholar.org/CorpusID:1221763>
- [33] K. Oldham and Spanier, *Atlas of functions: with equator, the atlas function calculator/* by Keith Oldham, Jan Myland and Jerome Spanier, 2nd ed. New York: Springer, 2009.